

Quantification of microplastics in a highway stormwater filter system and design of filter soil material based on a column infiltration experiments



Master's Thesis

Janka Kelényi

Water and Environmental Engineering
Aalborg University



AALBORG UNIVERSITY
STUDENT REPORT

Faculty of Engineering and Science

Department of Civil Engineering

Water and Environmental Engineering

Thomas Manns Vej 23

9220 Aalborg

<http://www.civil.aau.dk>

Title:

Quantification of microplastics in highway stormwater filter system and experimental soil composition

Theme:

Microplastic Pollution

Project:

MSc. 3rd and 4th semester

Project period:

September 2nd 2020 - Juni 10th 2021

Author:

Janka Kelényi

Supervisor:

Alvise Vianello

Co-supervisors:

Lucian Iordachescu

Jes Vollertsen

Abstract:

Stormwater ponds and filter installations can be used in stormwater management, but the microplastic retention capability of such an installation is unknown.

The purpose of the study is to analyse the microplastic retention efficiency and the accumulated microplastic concentration of the filter installation. The investigation was performed using samples from the file inlet and outlet water and soil samples from the filter installation. The samples were purified with a multi-step sample preparation process and were analysed using FPA- μ FTIR-imaging spectroscopy.

As a secondary purpose, different soil mixtures were used in an experimental setup to compare the soils' microplastic retention capability. The soil columns were spiked with with a known amount of microplastic which was counted with FlowCam equipment. After passing the water corresponding to the annual rainfall through the experimental column, the soil and water samples were purified and were analysed using FPA- μ FTIR-imaging spectroscopy. The used reference spectra library was compiled from the materials used for spiking.

Thesis report page: 57

Appendix: 1

Handed in: 10-06-2021

Preface

This report is a Master's Thesis written for the Environmental Engineering Master's program at Aalborg University. The project was carried out as a long dissertation during the period September 2, 2020 - Juni 10, 2021.

I want to thank my supervisor, Alvise Vianello, and Co-supervisor, Lucian Iordachescu and Jes Vollertsen, for their guidance, each of whom kindly shared their time, knowledge and experience during the project period.

I also want to express my gratitude to Claudia Lorenz, Rupa Chand, Fan Liu, Jeanette Lykkemark and Jytte Dencker for being helpful with the experimental work. Lastly, I want to thank my husband, Gyula, for supported me with love and understanding.

Aalborg University, June 10, 2021

Contents

Preface	iii
---------------	-----

I Introduction

1	Introduction	3
1.1	Project location	4
2	Purpose and Scope	5

II Filter system

3	Materials and methods	9
3.1	Sampling	9
3.1.1	Sampling strategy	9
3.1.2	Sampling locations, methods and tools	10
3.2	Sample processing	13
3.2.1	Soil sample preparation	13
3.2.2	Water sample preparation	20
3.3	Identification and quantification	23
3.3.1	Smaller than 500 μm particles	23
3.3.2	Larger than 500 μm particles	24
4	Results and discussion	25
4.1	Background contamination	26
4.2	Soil layer samples' results	26
4.3	Top soil samples abundance and polymer composition	28
4.4	Comparison of water samples' results	31
4.5	Follow-up experiment	32

III Filter soil experiment

5	Experimental method	35
5.1	Experimental setup	35
5.2	Column preparation	35
5.3	The experiment	36

6	Materials and methods	37
6.1	Materials	37
6.1.1	Filter soil mixtures	37
6.1.2	Plastic particle types and quantities	38
6.2	Sample processing	40
6.3	Identification and quantification	41
7	Results and discussion	43
7.1	Polymer distribution by column	43
7.2	Polymer distribution by polymer type	43
7.3	Polymer distribution by size	45
7.4	Follow-up experiment	47

IV

Conclusion & Reflection

8	Conclusion	51
8.1	Filter installation	51
8.2	Filter soil experiment	52
9	Bibliography	55
A	Experimental sample IDs	59



Introduction

1	Introduction	3
1.1	Project location	
2	Purpose and Scope	5

1. Introduction

After the discovery of plastics, their usage spread rapidly due to their good mechanical and utility properties such as light weight, durability and low production cost. This has led to a rapid spread of use and their production has multiplied, 1.5 million metric tons plastic was produced in 1950, while in 2019, 368 million metric tons of plastic was produced [Tiseo, 2021]. However, in parallel with the spread of plastic use, the plastic waste management lagged behind, causing an accumulation of discarded plastics in the environment. Plastic waste is not only burnt but dumped on landfills where it degrades, fragments, erodes into smaller pieces and as a result, secondary microplastics are generated. Another source of micro- and nanoplastics is when the microplastic particles have been intentionally made, these are known as primary microplastics. There is a lot of debate of which size ranges to include in the microplastics and nanoplastics definition, but with a size smaller than $0.1 \mu\text{m}$ are commonly defined as Nanoplastics (NP), and with the size between $0.1 \mu\text{m}$ and 5mm are the microplastics (MP) [Redondo-Hasselerharm et al., 2020]. This thesis deals with particles in the size range of microplastics.

Some of the created or produced microplastics travel in the air, the water or the soil, and then some are deposited in the water. The concentration of the MP and NP contamination is reportedly increasing in the freshwater systems, terrestrial habitats [Wagner et al., 2014] and oceans [ACD-GRI, 2019]. The aquatic environment is particularly affected by microplastics, as high-density plastic particles accumulate in sediments and low-density MPs float in the water body [Avio et al., 2017]. Aquatic organisms confuse plastic with food, which accumulates in their bodies and exerts its harmful effects such as malnutrition, physical damages and ingestion resulted ecotoxicological effects [Avio et al., 2017]. However, it not only has a detrimental effect on a consumer organism, but it affects all aquatic organisms through the food chain (bioaccumulation). Taking the negative effect into consideration, efforts should be made to retain as many microplastics as possible.

As a consequence of human development and growth, it is common that contaminants coming from urban areas find their way into the aquatic environment. The microplastics in the roadwater runoff may originate from car tyres, road de-escalation, vehicles, resting facilities, littered waste and atmospherically deposition. The roadwater runoff is reportedly a pathway of the microplastics to the aquatic environment [Horton et al., 2017]. In order to protect the sensitive recipient, the runoff water polishing can be typically done with filters.

This study is performed as an extension of a project where the installed filter system at the Herning Motorway [Vollertsen et al., 2018a] was examined on how the sub-elements of the filter installation are effective at withholding microplastics. The filter system consists of a stormwater pond and a soil filter. Based on the article Liu et al. [2019], the stormwater retention ponds withholds a significant proportion of microplastics so these can be considered pollution hot-spot and they contribute in transport between urban areas and the aquatic environment.

This study examines the filter basin retention capability and only as a source take into consideration the pre-basin's water. In addition, small scale prototypes of different potential filter soil mixtures

were set up to develop an optimal filter soil for micro-plastic retention.

1.1 Project location

The tested filter system is located next to road 15 (motorway from Aarhus to Silkeborg, Herning motorway), west of Låsby, located in the immediate vicinity of a gas station. Figure 1.1 shows the satellite view of the filter system where the primary recipient of the runoff is the stormwater pond. The catchment area of the inflowing water consists of road areas [Vollertsen et al., 2018a]. The water of the soil filter treating runoff drained from the stormwater pond. The water treated by the lake enters the filter installation through the overflow of the lake.

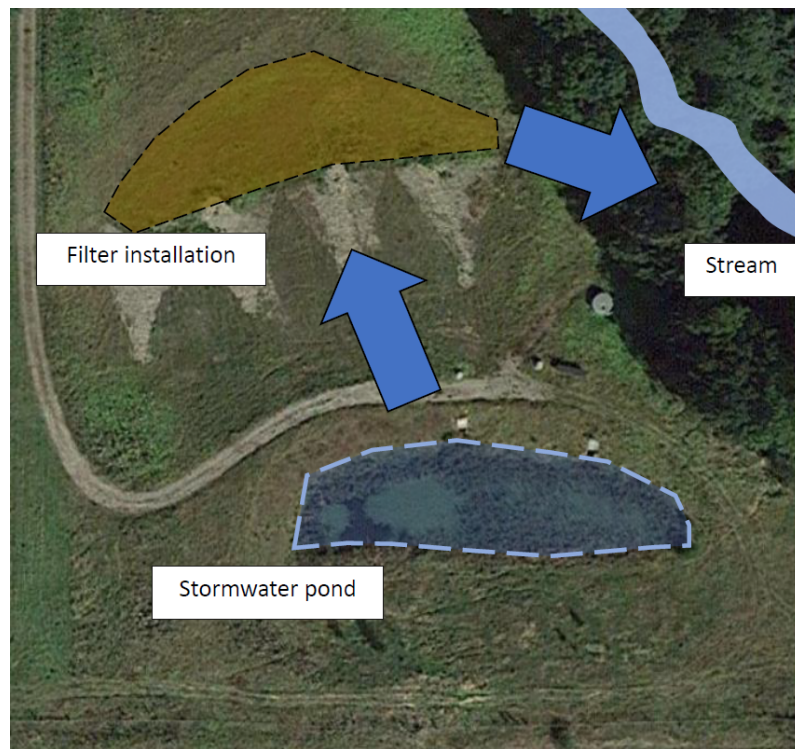


Figure 1.1: *Satellite view of the filter system*

The filter installation (see Figure 1.2) consists of a layer of 0.3 m of sand (filter sand 0/4, Dansand) mixed with 5 % w/w peat, followed by 1 meter of limestone and finally 0.2 meter of thick drainage sand. A synthetic sheet is placed between the layers of the filter [Vollertsen et al., 2018a].

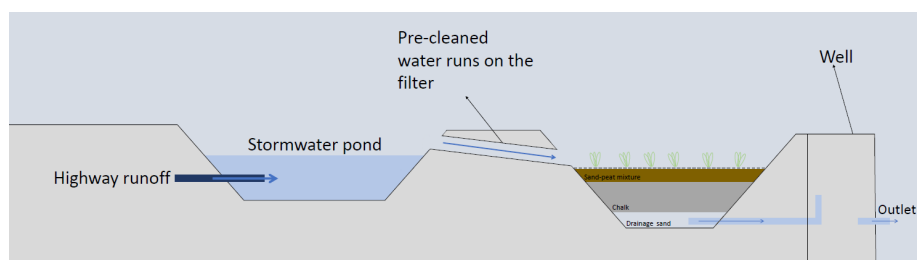


Figure 1.2: *Schematic of the filter installation [Vollertsen et al., 2018b]*

2. Purpose and Scope

The research in this thesis has been performed from 2019 September to 2020 June. The study was divided into two parts and the project strategy was created accordingly. In Denmark, a large fraction of the urban runoff is treated with the use of stormwater ponds which is the most widely used practice for stormwater management. This study quantifies and identifies the microplastics in the filter installation, The filter soil system retention capability was evaluated by investigating the water from the pond and the outlet of the filter. In order to be able to design a filter soil layer which is more effective in retaining microplastic particles, an experiment was set up where soils with different grain sizes' retention capability was compared.

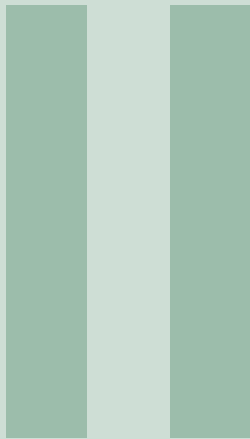
This leads to the following questions:

Does the soil-filter basin remove and/or retain microplastic pollution from the incoming wet basin pre-treated road water? How effective is the filter basin in removing and/or retaining microplastic pollution? What is the actual accumulated concentration in the filter surface?

To answer the first question, soil samples were taken from eight sampling points and water samples were collected at the inlet and outlet of the filter installation. Additionally, in parallel with the water samples, blank samples were taken to account for the atmospheric deposition of microplastics. The samples were analysed with FTIR spectroscopy.

How can different soil mixtures capable to remove and/or retain microplastic polluted water? How far down can the microplastic penetrate the different soil filter materials? How thick filter layer is needed to protect the sensitive recipient?

To answer the remaining research questions formulated previously, six different soil mixtures were created and used with a column experimental laboratory setup. Plastic particles with known quantity and quality were added to the columns. The experiments resulted in 3 soil and 1 water sample per designed filter soil. The plastic particles that were introduced in the system, were counted with FlowCam machine and the samples were analysed with FTIR spectroscopy.



Filter system

3	Materials and methods	9
3.1	Sampling	
3.2	Sample processing	
3.3	Identification and quantification	
4	Results and discussion	25
4.1	Background contamination	
4.2	Soil layer samples' results	
4.3	Top soil samples abundance and polymer composition	
4.4	Comparison of water samples' results	
4.5	Follow-up experiment	

3. Materials and methods

3.1 Sampling

3.1.1 Sampling strategy

Soil and Inlet water samples

The first soil samples (Sample point number 0 see Figure 3.2) were taken on 25 August 2020 and the rest of the soil samples and the inlet water samples were taken during dry weather on 22 September 2020. Dry weather means no rain event or maximum of 3 mm precipitation for two days before and during sampling.

Outlet water samples

The outlet water samples were not taken at that time because the well did not contain enough water ($3 \times \sim 1m^3$) to be able to take the samples. In order to sample the required amount of water, the inlet of the filter soil (the outlet of the lake) was closed on 22 September. The outlet water samples were taken after the wet weather period on 5 November, 2020. Wet weather means multiple rain event two weeks before sampling.

Due to the multiple rain event, the water level of the stormwater pond was significantly increased. To have enough water in the well, the lake drain sluice was opened for around 2 minutes in every second hour and in the middle of the last outlet water sampling the gate was left open and the soil filter system was flooded. Due to the high flow rate, the particle content of the outlet water was increased, and the metal filters were clogged during the last outlet water sampling.



(a) Water flow with opened stormwater pond outlet

(b) Flooded filter soil system

Figure 3.1: *Filter soil during and after flooding*

3.1.2 Sampling locations, methods and tools

In order to get the soil and the water samples, two different sampling method were applied. For clear identification, the samples were named according to the following principle:

Sample location - Sample type - Number of the sampling point or the sample - Sample source

Soil samples

Soil samples were collected from eight points of the filter soil system. The location of the sampling points can be seen in Figure 3.2.



Figure 3.2: Filter soil sampling points

The soil samples from the sampling point 1-7 were taken in the upper 5 cm of the filter soil system. 1-4 the sampling points are located at the line of the inlet pipe, right after the gravel section ended and the sandy section started. The samples from sample point number 0 were taken from 3 different layers where the top layer was the first 10 centimetres from the surface, the bottom layer was between 10 and 20 cm and the bottom layer was from 20 to 25 cm, where the filter soil system membrane was unearthed. The sampling point is located just beneath the mouth of the inlet pipe. The main information of the soil samples can be seen on Table 3.1.

Table 3.1: *The collected soil samples' ID according to the sample location, sample type, sampling point and sample source.*

Sample ID	Location	Type	Sampling point	Source
LS0T	Lasby	Soil	0	Top layer: 0-10 cm
LS0M	Lasby	Soil	0	Middle layer: 10-20 cm
LS0B	Lasby	Soil	0	Bottom layer: 20-25 cm
LS1T	Lasby	Soil	1	Top layer: 0-5 cm
LS2T	Lasby	Soil	2	Top layer: 0-5 cm
LS3T	Lasby	Soil	3	Top layer: 0-5 cm
LS4T	Lasby	Soil	4	Top layer: 0-5 cm
LS5T	Lasby	Soil	5	Top layer: 0-5 cm
LS6T	Lasby	Soil	6	Top layer: 0-5 cm
LS7T	Lasby	Soil	7	Top layer: 0-5 cm

In order to have a representative sample, 1 m^2 area was defined as sampling point where the vegetation was removed by hand and shovel. The samples were taken with a spoon while plants and roots were avoided. To prevent contamination, plastic-free and metal paint-free tools were used.

The soil samples were placed in a glass container, sealed and labelled. Until processing, the samples were stored in a cold room at a temperature ranging from -2°C and 5°C .

Water samples

Water samples were collected with a custom made plastic free pump-fed filtering device (UFO system - Universal Filtering Objects system [Rist et al., 2020]). The flexible metal hose was submerged under the water surface. In case of the stormwater pond water sampling, 5 mm mesh size metal cage was used at the inlet in order to protect the system against large particles. During the well sampling, this protection was not necessary. The water entered to the modular filtering unit through the hose with the inverter-controlled pump. The filtering unit consists of three parts, where 300 μm metal filter was used at the first unit and 10 μm mesh sized metal filter was inserted to the second and third unit. The larger mesh sized filter is used to delay the clogging of the finer filters. The filtering system is built almost entirely out of metal, where only the gasket is made of silicone. The water path is split after the unit containing the large mesh filter and filtered parallelly in the two fine filter containing units. The filtered water leaves the system through the inbuilt flow meter and outlet hose. The flow meter is used to determine the amount of filtered water.

The three parallel filter soil's inlet water samples were taken from the stormwater pond's outlet area (see Figure 3.3a) and the three parallel outlet water samples were taken at the sampling well (see Figure 3.3b).



(a) Soil filter system inlet water sampling point (Stormwater pond outlet) (b) Soil filter system outlet water sampling well

Figure 3.3: *Water sampling points*

At first, the UFO system was primed with the sampling points' respective water (in case of the inlet sampling with the pond water, in case of the outlet sampling with the water from the well) to flush the system of potential plastic particles retained in the pipeline. This operation was done before placing the filters inside the UFO units. Subsequently, approximately 1 m^3 of water was filtered per sample. After sampling the filtration system was emptied with a compressor. The filtration units were opened and the stainless-steel filters were removed/replaced. The used $300\ \mu\text{m}$ and two $10\ \mu\text{m}$ filters were placed into petri dish, labelled, wrapped with aluminium foil and labelled.

Blind samples were also taken during water sampling in order to account for the air-born micro plastic contamination during the sampling process. An empty petri dish was opened while the UFO system was open, and the metal filters were exposed to the environment related contamination. Separate air-blanks were taken during the inlet and the outlet sampling. The blank samples were packed and labelled as the water samples.

The collected water and blind samples can be seen in Table 3.2. The samples were stored in cold room until processing.

Table 3.2: *The collected water samples' sample size and IDs according to the sample location, sample type, sampling number and sample source.*

Sample ID	Location	Type	Sample number	Source	Size [m^3]
LW1I	Lasby	Water	1	Inlet	1.116
LW2I	Lasby	Water	2	Inlet	1.424
LW3I	Lasby	Water	3	Inlet	1.157
LWBI	Lasby	Water	Blank	Inlet	N/A
LW1O	Lasby	Water	1	Outlet	1.033
LW2O	Lasby	Water	2	Outlet	1.008
LW3O	Lasby	Water	3	Outlet	0.796
LWBO	Lasby	Water	Blank	Outlet	N/A

3.2 Sample processing

In order to extract the microplastics from the water and soil samples, an multi-step extensive purification method was used. The removal of these materials is crucial to ensure an accurate analysis, extracting the potential MPs particles from the matrix, simultaneously concentrating the sample .

In order to reduce the risk of contamination during the sample processing, several precautions were implemented. First of all, plastic tools were avoided in favour of stainless steel lab tools, all glassware was flushed three times with filtered demineralized water (filtered with a $0.7 \mu\text{m}$ glass fibre filter) before use and a cotton lab coat was worn during all operations. Secondly, the used reagents were filtered with $0.7 \mu\text{m}$ glass microfiber filter before use and the containers were covered with aluminium foil or glass lids. Furthermore, to prevent cross-contamination and sample loss, the same $10 \mu\text{m}$ steel filters were used for each of the filtration steps for one sample. Between the filtration steps the metal filters were stored in closed petri dishes. In case of the sample transfer, and to avoid sample loss, the original container was flushed three times. In addition, the majority of the sample preparation process was performed in a fume hood in order to prevent contamination.

3.2.1 Soil sample preparation

The general overview of the soil sample preparation can be seen on Figure 3.4. The sample processing was performed based on Löder et al. [2017], the process steps are described in the continuation of the chapter.

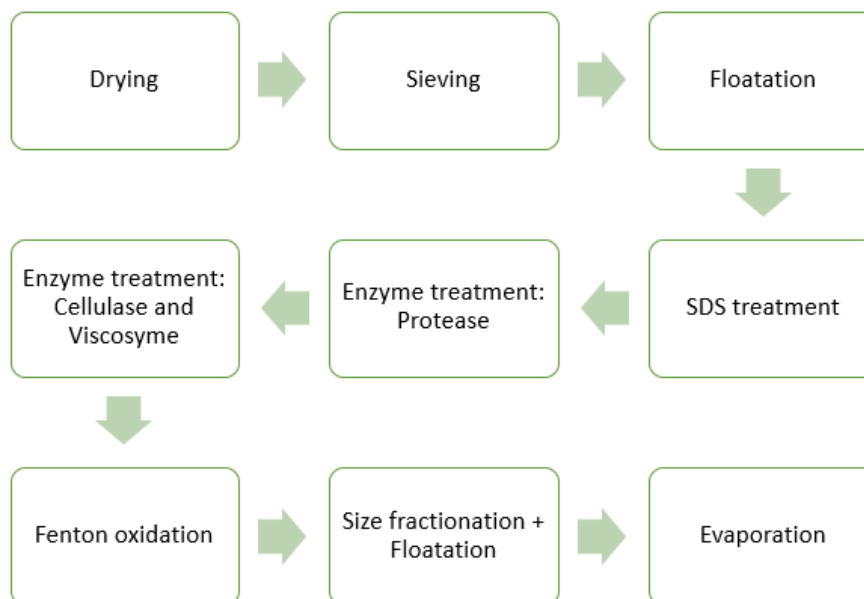


Figure 3.4: Flowchart of the soil sample preparation

Drying and Sieving

The samples were placed in the oven to dry with aluminium foil cover. The temperature was set at 60°C, a suitable temperature to slowly evaporate water without damaging the microplastic particles. The dry samples were gently homogenised by using a mortar to break up the aggregates and ~ 300 g of sample was weighed out. The exact amount of the samples are shown in Table 3.3.

Table 3.3: *Sample size.*

Sample ID	Sample size [g]	Sample ID	Sample size [g]
LS0T	300.02	LS3T	300.01
LS0M	300.06	LS4T	300.01
LS0B	280.34	LS5T	300.02
LS1T	300.03	LS6T	300.00
LS2T	300.02	LS7T	300.01

The measured samples were sieved through 1 mm sieve by means of a sieve shaker (Retsch AS 200 control, Retsch GmbH) for 20 minutes with the amplitude of 0.7 mm / "g" (see Figure 3.5a). As a result, the sample was separated to larger and smaller than 1 mm sample fractions (see Figure 3.5b).



(a) Sieve shaker with the sieving tower



(b) The larger and the smaller than 1 mm sample fractions (LS4T)

Figure 3.5: *Sieving setup and the sieved sample fractions*

The fraction larger than 1 mm was labelled and stored in closed container until analysis. The finer fraction (< 1 mm) was used for further sample processing. The separation of the fraction is necessary so that it does not exceed the diameter of the separating funnel's tap used during the density separation process and thus does not cause a problem during the release step.

Floatation

Pre-oxidation was not necessary, because the samples were taken from an artificially created soil layer with 95% coarse sand and 5 % peat. This organic matter content does not require a pre-oxidation step.

Density separation was used to separate the microplastics from the inorganic part of the sample matrix. During the floatation process, the denser particles sink to the bottom and the less dense particles float on the surface of separation liquid.

To separate the soil mixtures components based on their density, dissolved sodium polytungstate (SPT) powder and separation funnel was used. SPT is suitable for heavy liquids separation because it has high solubility in water with the maximum density of $3.1 \text{ g} \cdot \text{cm}^{-3}$. The advantageous property of the substance is that it is non-toxic, and it has relatively low viscosity [Munsterman & Kerstholt, 1996]. However, it is expensive, so the used SPT solution was recovered with filtration.

In order to define the most suitable SPT density, the samples from the sample point 0 were processed with different SPT densities. The top soil layer was processed with SPT $1.7 \text{ g} \cdot \text{m}^{-3}$, the middle layer with $1.6 \text{ g} \cdot \text{m}^{-3}$ and the bottom layer with $1.5 \text{ g} \cdot \text{m}^{-3}$.

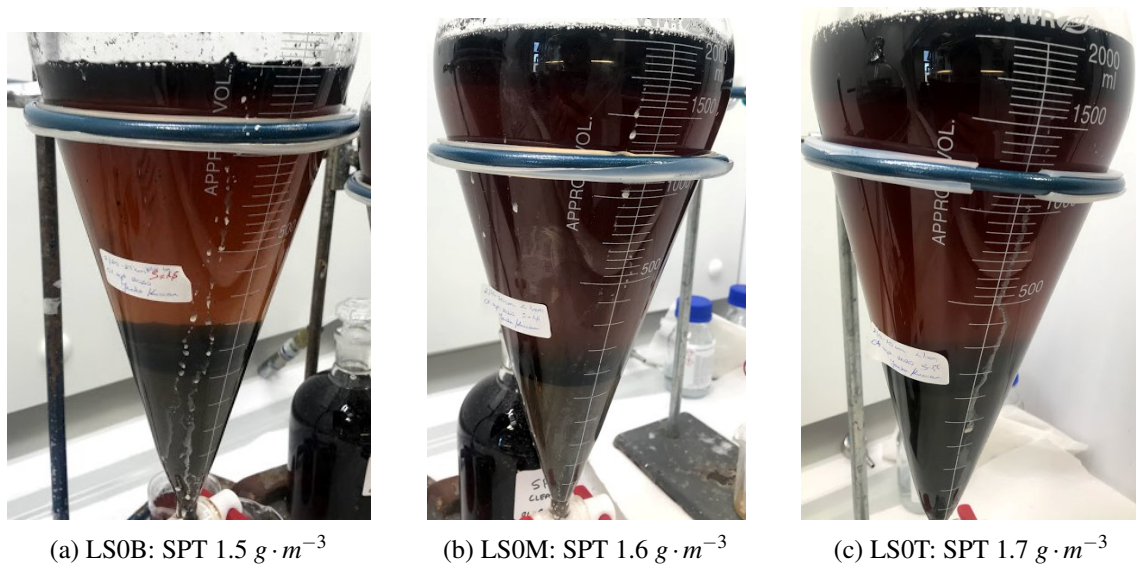


Figure 3.6: Density separation of samples from sampling point 0 with different SPT density

Figure 3.6 shows that, the first funnel with the lowest density has the largest amount of deposited material and the least amount of floating material. The floating material's volume increasing with the increasing density. Therefore, the sample preparation is less troublesome in lower densities, because most of the particles are sedimented and proceeded only the lightest, floating particles.

Since the activities carried out in this master thesis are part of a wider project targeting also the retention of car tire particles by the filter system, the sample extraction, and specifically the floatation step, had to consider this specific target material. Therefore, a further evaluation was required to define the SPT density suitable for the sample while the car tire particles are recovered. The experiment was performed with clean (not used) car tire particles of $20\text{-}500 \mu\text{m}$ in size and with SPT in density $1.5 \text{ g} \cdot \text{m}^{-3}$, $1.7 \text{ g} \cdot \text{m}^{-3}$, $1.9 \text{ g} \cdot \text{m}^{-3}$ and $2.1 \text{ g} \cdot \text{m}^{-3}$.



Figure 3.7: Car tire density experiment. The density values from left to right: $1.5 \text{ g} \cdot \text{m}^{-3}$, $1.7 \text{ g} \cdot \text{m}^{-3}$, $1.9 \text{ g} \cdot \text{m}^{-3}$, $2.1 \text{ g} \cdot \text{m}^{-3}$

Figure 3.7 shows that the pure car tire particles are floating at all experimental densities so that it can be concluded, the tested particles' density is less than $1.5 \text{ g} \cdot \text{m}^{-3}$. However, the tire and road wear particles (TRWP) are heavier than the pure car tire particles. In order to keep 90% of TRWPs in the processed samples while the density kept as low as possible, $1.9 \text{ g} \cdot \text{m}^{-3}$ density need to be used during the density separation process [Klößner et al., 2019].

In order to process $\sim 300 \text{ g}$ sample, 2000 ml separation funnel was used for density separation. The sample was transferred to the separation funnel with SPT solution and the funnel was filled up with SPT until it reached the 1500 ml mark. An air supply was connected to the bottom of the funnel, and the content of the funnel was aerated to mix properly the solid and liquid fractions for 15 minutes. After bubbling, the inner wall of the separation funnel was flushed with SPT with adequate density and filled up until it reached the largest aperture of the funnel. The SPT densities used for sample processing are shown in the table can be seen in Table 3.4. The setup was left to settle overnight. Subsequently, the sediment was removed from the bottom of the funnel by opening the stopcock, and the procedure was repeated once more to ensure a better extraction of the potential MPs.

Table 3.4: Used SPT density values.

Sample ID	SPT density [$\text{g} \cdot \text{cm}^{-3}$]	Sample ID	SPT density [$\text{g} \cdot \text{cm}^{-3}$]
LS0T	1.7	LS3T	1.9
LS0M	1.6	LS4T	1.9
LS0B	1.5	LS5T	1.9
LS1T	1.9	LS6T	1.9
LS2T	1.9	LS7T	1.9

After a second overnight settling step, the sedimented particles and $\sim 1500 \text{ ml}$ SPT were discharged. The rest of the SPT with the floating fraction was filtered with a $10 \mu\text{m}$ mesh sized metal filter.

SDS treatment

The filters with the samples was sonicated in and the tools were flushed with 5 % Sodium dodecyl sulphate (SDS) solution. The SDS solution was used as a detergent to denature, extract and solubilize proteins. SDS is an anionic detergent which is capable to unfold most protein structures and to render them to polypeptides [Kurien et al., 2019]. With SDS treatment the organic residues'

contact surface was increased, thereby the following enzymatic reactions' efficiency were increased. [Löder et al., 2017]

250 ml 5% SDS solution was incubated with the sample overnight at 50°C in a magnetic-stirred water bath (150 rpm).



(a) After floatation, before SDS treatment



(b) After SDS treatment

Figure 3.8: *The filtered sample changes appearance as a result of SDS treatment*

The result of the SDS treatment can be seen in the comparison of the filtered sample material before and after SDS treatment. On figure 3.8a small roots and particles can be seen. However, after the SDS treatment the larger particles fragmented to small particles and the filtered sample looks more homogeneous in size (see Figure 3.8b).

Enzyme treatment: Protease

After the overnight incubation with SDS, - similarly to the previous step - the sample was filtered onto a 10 μm mesh sized metal filter, which was rinsed with 250 mL of tris-(hydroxymethyl)-amino-methane (TRIS) buffer and then briefly sonicated (5 minutes).

As first enzymatic treatment, protease was used to increase the speed of protein chains' decomposition [Löder et al., 2017]. To ensure an optimal environment for the enzymatic reaction with 0.5 ml of protease (Protease from *Bacillus* sp. liquid, ≥ 16 U/g, SIGMA), the TRIS solution was used with a pH of 8.2. The sample was incubated in a water bath at 50°C for at least 40 hours while stirred at 150 rpm.

Enzyme treatment: Cellulase and Viscosyme

After incubation, according to the procedure described earlier, the sample was filtered, and flushed from the filter into a beaker with 250 ml acetate buffer to provide the optimal 4.8 pH level for the next enzymatic reaction. Cellulase (SIGMA, Cellulase, enzyme blend) and viscosyme (SIGMA, Viscosyme®L, Cellulotic enzyme mixture) enzymes were indeed used to decompose cellulose and pectin-like molecules, thereby hydrolyse the polysaccharides in the cell wall [Fang & Qu, 2018].

The sample, spiked with 0.5 ml cellulase blend and 0.5 ml viscosyme enzyme was incubated at least 40 hours in 50°C water bath with 150 rpm stirring.

Fenton oxidation

After at least 40 hours incubation, the sample was filtered onto 10 μm mesh sized metal filter, the filter was sonicated and flushed with 200 ml filtered demineralized water.

Fenton oxidation was used in order to effectively decompose the organic compounds in the sample, where a catalyst (62 ml 0.1 M iron sulphate ($\text{FeSO}_4 \cdot 7\text{H}_2\text{O}$)) was used to accelerate the oxidative

effect of the non-selective oxidant (145 ml hydrogen peroxide (H_2O_2)). As a result of the reaction hydroxyl and hydroperoxyl radicals are generated: [Tagg et al., 2017]



In order to have proper and controlled reaction, the pH level was increased with a strong base (65 ml 0.1 M sodium hydroxide (NaOH) solution). The reaction under less acidic conditions slows down, because the reaction speed depend on the ferric ion (Fe^{3+}) concentration. Under high pH conditions the Fe^{3+} concentration is lower, because its concentration is depend on the ions solubility which is depend on the pH. Thus, when NaOH was added, Fe^{3+} is precipitated as Iron(III) oxide-hydroxide ($Fe(OH)_3$) and the reaction slowed down [Xiao et al., 2016]. The target pH was in case of Fenton oxidation is pH 3 [Rasmussen et al., 2021].

In addition, Fenton oxidation is rapid and exothermic reaction, where higher temperature cause enhanced decomposition and lower temperature cause less intense reaction [Zazo et al., 2011]. So in order to have an optimal breakdown process, the temperature of the reaction was monitored with core thermometer and kept between 20-30 °C with ice-water bath. If the temperature was too high, ice was added to the water bath, and if the temperature was too low, it was removed from the water bath.

Despite the temperature and pH-controlled reaction, excessive foaming of the sample may occur. To avoid sample loss, the foam can be crushed with filtered water, while being careful to avoid over-dilution which can have negative effects on the reaction. In addition, during the reaction stirring was avoided as it may adversely affect the reaction. The sample was let to stand overnight.



(a) After enzyme treatments, before Fenton oxidation



(b) After Fenton oxidation

Figure 3.9: The filtered samples change appearance as a result of Enzyme treatments and Fenton oxidation

The result of the Fenton oxidation can be seen in the comparison of the filtered sample material before - and after Fenton oxidation. On figure 3.9a small particles are present. However, after Fenton oxidation the small particles fragmented to tiny particles and the filtered sample looks homogeneous in size (see Figure 3.9b).

Size fractionation and Floatation

The oxidized sample was wet-sieved with a 500 μm mesh sized metal sieve. The size fractionation is performed in order to remove the larger particles than 500 μm , because those are too thick to analyse with μFTIR -Imaging.

The fraction larger than 500 μm was back-flushed with filtered demi-water into a glass beaker. The beaker, covered with alu-foil, was placed to the oven to dry at 55°C. The smaller than 500 μm fraction was filtered with 10 μm mesh sized metal filter. The sample on the filter was sonicated in 1,9 $\text{g} \cdot \text{m}^{-3}$ SPT solution and transferred to 250 ml separation funnel. The funnel was filled with SPT until it reached the 3/4 of the funnel. After 15 minutes of aeration the sample was left to settle overnight. The purpose of this floatation process is the same as described in Floatation section. Accordingly, after the overnight settling the settled material was removed. The aeration, overnight settling and settled material removal were repeated 2 times.



Figure 3.10: *Floatation of top soil samples*

In Figure 3.10 the soil samples can be seen after the first overnight settling. The samples behave noticeably differently, the sample in the 1st (LS1T) and 5th (LS5T) funnels already separated after the first treatment with a small floating and a larger amount of sedimented fraction. In case of the 4th funnel (LS4T) the fractionation is not complete, the middle section is not clear, so it is still containing particles with different densities. The density separation in the other funnels (2nd - LS2T, 3rd - LS3T, 6th - LS6T, 7th - LS7T) are also not complete. In that cases the ratio of the bottom and floating section is not optimal, the floating section usually a small layer. It means that the floating part still contain larger than 1,9 $\text{g} \cdot \text{m}^{-3}$ density particles, so further mixing and settling was required to separate them.

Evaporation

After the last overnight settling, the settled material removal was repeated in every 30 minutes until there was no settled material. The rest of the SPT with the floating fraction was filtered onto a 10 μm mesh sized metal filter. The sample was flushed with 1 litre 50°C filtered demi water and 100 ml 50 % EtOH to remove the leftover SPT residues from the sample. The SPT residue in the deposited sample forms yellow crystals which cause difficulties during the FTIR analysis.

The filtered sample transferred to 50 % EtOH solution and evaporated in 5 ml vial with 55°C water bath with nitrogen flow. The nitrogen flow is 0.8 l/min for 10 minutes, after that 1.2 l/min for

20 min, finally 1.8 l/min for 120 min. With these flow values at the beginning, when the vial is almost full, the flow does not blow out the sample from the vial. The flow rate increasing in order to increase the evaporation's efficiency while the sample loss is avoided. After evaporation of the entire sample, 5 ml of 50 % EtOH was added using a calibrated glass pipette. The vial closed with a silicone stopper and cap. The vial was sonicated for 5 minutes in order to remove the particles clinging on the wall.

Transfer

At first, the clean compression cell and the 2 mm thick zinc selenide transmission window with 13 mm diameter (10 mm active diameter and 78.5 mm^2 active area) was assembled (see figure 3.11a). After that the sample was mixed with vortex mixer and 50 or 100 μl sample was taken with a disposable glass capillary micropipette and deposited on the transmission window (see figure 3.11b). In order to evaporate the 50 % EtOH, the compression cell with the sample was placed on a 55°C heating plate. To avoid the contamination of the sample during the drying process, the transmission window was covered with a small beaker.

As soon as the sample is dry, the transmission window was inspected with microscope to check the particle population and distribution. If necessary, additional sample was deposited.



(a) Preparation for deposition



(b) The deposited sample

Figure 3.11: *The sample transfer and deposition*

3.2.2 Water sample preparation

The water sample purification steps were performed in Laminar Air Flow (LAF) cabinet and cotton clothing was worn to prevent contamination.

For the water samples a shortened sample preparation method was used (see figure 3.12). The process steps are described in the continuation of the chapter.

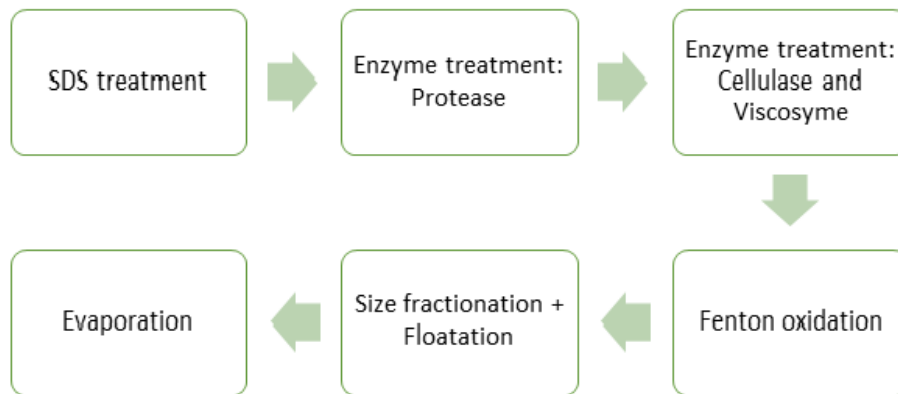


Figure 3.12: *Flowchart of the water sample preparation*

SDS treatment

The sample containing filters from the UFO system were placed separately in a crystallizer with 5 % SDS solution. The particles were removed from the filter with 5 minutes sonication in an ultrasonic bath, the filter was scraped with spatula and flushed, and the sample was transferred into a 1 liter beaker. The incubation process was performed identically as the soil sample's SDS treatment.

On figure 3.13 the inlet (Figure 3.13a) and outlet (Figure 3.13b) water and blank samples' appearance can be seen after the SDS treatment. It is obvious that although the 3 inlet and the 3 outlet sample are parallel samples, the samples are different in appearance.



(a) Inlet water samples and blank sample - After SDS treatment



(b) Outlet water samples and blank sample - After SDS treatment

Figure 3.13: *The water samples appearance after SDS treatment*

Enzyme treatment: Protease

In case of the inlet water samples the protease enzyme treatment performed identically such as the soil samples. In case of the outlet water samples the protease treatment was not performed.

The inlet water samples appearance can be seen on Figure 3.14, showing that the samples became visibly lighter.

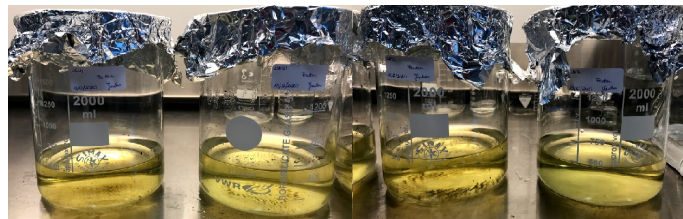


Figure 3.14: *Inlet water samples appearance after the protease enzyme treatment*

The rest of the sample preparation followed the same steps performed as for the soil samples preparation.

Fenton oxidation

To follow the change of the appearance of the inlet and outlet water samples, Figure 3.15 shows the samples after Fenton oxidation. The lightening of the sample indicates that the sample mass and the concentration of particles are decreasing.



(a) Inlet water samples and blank sample - After Fenton oxidation



(b) Outlet water samples and blank sample - After Fenton oxidation

Figure 3.15: *The water samples appearance after Fenton oxidation*

Size fractionation and Floatation

During floatation, 100 ml separation funnel was used in case of the inlet water samples and 250 ml in case of the outlet water samples. The sample preparation result and the reduction of the sample mass can be seen on Figure 3.16. A purified sample was obtained as a result of sample preparation.

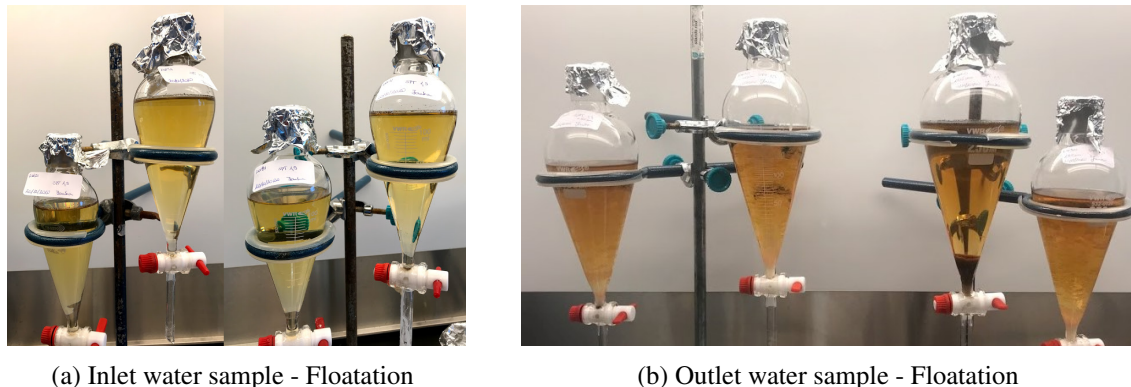


Figure 3.16: *The water samples appearance during floatation*

3.3 Identification and quantification

3.3.1 Smaller than 500 μm particles

To identify the particles in the sample on the ZnSe window, Cary 620-670 FTIR system (microscope and spectrometer, Agilent Technologies) was used with a 15x visible and IR objective (Cassegrain) and with Mercury–Cadmium–Telluride 128x128 pixel FPA detector (Agilent Technologies). The Fourier Transform Infrared (FTIR) spectrometer works with infrared spectroscopy, which measures the vibration of molecules in wavenumber per cm unit. Each material has a unique spectrum, therefore, the chemical composition of a substance can be determined with a comparison with an appropriate reference library.

The deposited particles on the transmission window were analysed in transmission mode. The scans resulted with an optical microscope picture and an IR field of view with 704 μm x 704 μm size where the IR pixel size was 5.5 μm x 5.5 μm (128 x 128 pixels per tile). The transmission wavenumber range was from 850 to 3750 cm^{-1} with a spectral resolution of 8 cm^{-1} . Before testing the sample, background check was performed. The numbers of scans were 30 in case of the sample and 120 in case of the background with 50 % beam attenuation. As the scan was performed in transmission mode, the results were in percent transmittance where the data range is between 0-100.

In order to analyse the maps from the μFTIR imaging, the SiMPle software was used [Primpke et al., 2020]. The software compares the IR spectrum of the pixels on the map with the spectra of the reference spectra database [Liu et al., 2019]. As a result, the algorithm generates the coordinates of the particles in pixels and in μm , the maximum score of the match with the reference library's materials, the group of the plastic, the major and minor dimension in μm , the feret min in μm , the particle volume in μm^3 and the particle mass in ng.

The analysis of the maps was performed at first with a reference library which contained 113 reference spectra of plastics and organic materials (absorbance). The reference library contains information about the material group's wavenumber, the threshold and the material density. The thresholds were manually set to determine the level of the match to reliable particle identification [Liu et al., 2019]. The material density was set based on the material's property for the volume to be calculated.

4. Results and discussion

During the manual evaluation of the particles defined as PE particles' spectra, difference was observed. Due to the similarity of the PE and the peat and fatty acid residues, most of the particles were misidentified as PE. In order to avoid the unreliable identification of the plastic particles, re-evaluation was performed with an extended reference library with 125 reference spectra where the peat and fatty acid residue spectra were added.

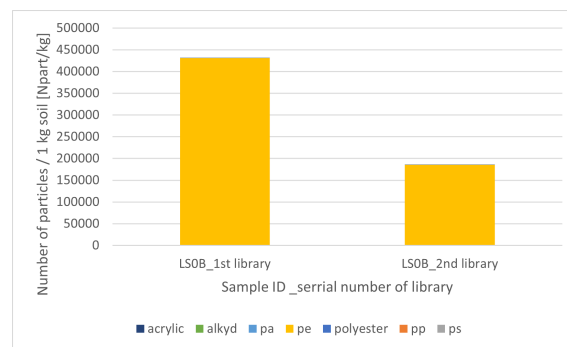


Figure 4.1: The MPs concentration by plastic type with the different reference libraries

Based on Figure 4.1, the decrease in the concentration (Npart/kg) of the PE particles is noticeable. In case of the LS0B sample, 431,262 particles were identified as PE particle with the library without peat and fatty acid spectra, and 185,846 particles with the extended library. It means that the second library resulted the elimination of significant amount of non-real PE particles. However, during the manual examination of the spectra, differences were noticed, which means that non-real PEs are still identified as PE particles (see Figure 4.2).

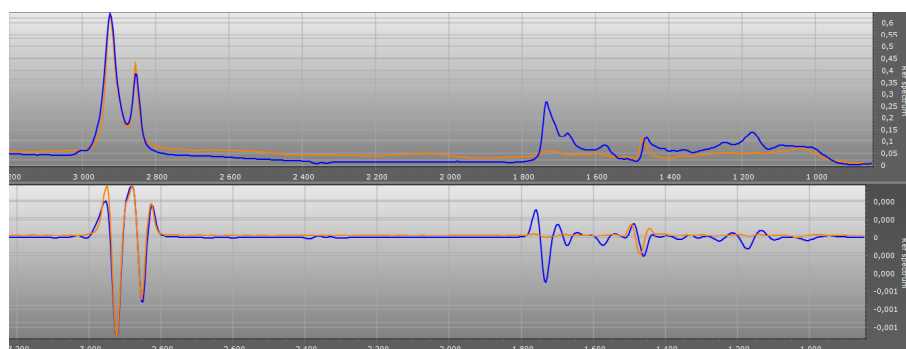


Figure 4.2: PE and non-real PE spectra - example

The identified difference at the lower wavelength section gives the possibility to improve the algorithm of the evaluation software. Nevertheless, the issues related to the misidentification of interfering materials as PE particles remained relevant, therefore, the PE data were excluded from the results.

4.1 Background contamination

The blank samples were collected while sampling the inlet and the outlet water samples and followed the same sample treatment. As result, 33 particles were found in the inlet and outlet water blank samples, while in average 6595 particles were found in the soil samples, which means 0.5 % contamination rate. In case of the water samples with lower MP concentration, the contamination rate is higher, 34 % in case of the inlet and 41 % in case of the outlet water samples.

In inlet water blank sample all the particles were polyester particles, while in case of the outlet blank samples, 50 % was polyamide and 50 % was polyester (see Figure 4.3).

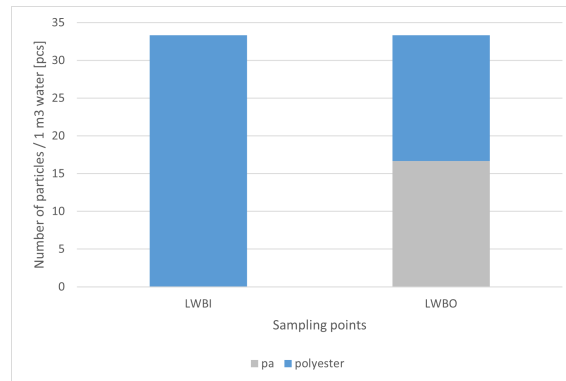


Figure 4.3: Polymer distribution in the blank samples based on the particle numbers.

In addition to the number of the particles, the major and minor dimensions were checked. Based on the dimensions of the particles the volume values were estimated. The mass of the particles was estimated based on the volume of the particles and the density of the polymer type.

The blank sample results were used to correct the MPs concentration in the samples, accounting for field and lab contamination. The number, the volume and the mass of the particles from the blank samples were subtracted from the sample results. When the result would be minus, the result was forced to zero.

4.2 Soil layer samples' results

The soil samples from sampling point 0 were evaluated in order to see the distribution and the retention of polymers in the different layers of the filter system. On figure 4.4 the number of polymer particles can be seen per 1 kg soil where the blank sample results were deducted.

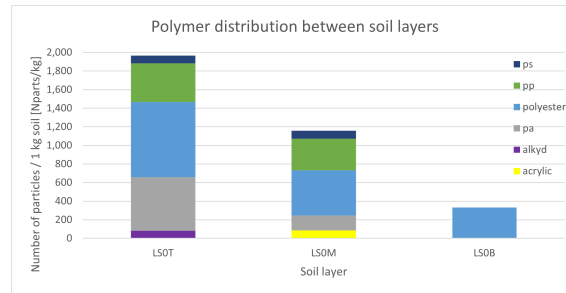


Figure 4.4: *MPs concentration (Npart/kg) and polymer composition of the three soil layers*

On Figure 4.4 the decreasing concentration (Npart/kg) of plastic particles can be by increasing depth. From plastic type point of view a different trend can be seen. In the top- and the middle layer the polymer composition is similar, but in case of the bottom layer only polyester particles were found. There may be several reasons for the presence of the polyester in the bottom layer. One of the reasons can be the contamination of the raw material which could have happened in several points, for example when it was brought out, during the machine mixing process, during storage in plastic bags, and while it was handled and transported by various means. Another reason might be that the filter construction includes a layer of geotextile, which might contain polyester particles. So the found concentration of polyester might well have been present in the filter material when the filter was being installed. It is hence not unlikely, that the complete filter soil had this polyester content already when it was constructed.

The difference in the retention can be caused by the difference in the particles densities where the polyester density is higher ($\sim 1,37\text{g} \cdot \text{cm}^{-3}$) than the density of polyamide ($\sim 1.08\text{g} \cdot \text{cm}^{-3}$), polypropylene ($\sim 0.9\text{g} \cdot \text{cm}^{-3}$) and polystyrene ($\sim 1.05\text{g} \cdot \text{cm}^{-3}$). However, the density of the plastic particles is not the only factor that affects the distribution of polymers between the soil layers. On Figure 4.5 the dimensions of the polymers per soil layer was plotted. It can be seen, the particles in the top soil layer are larger and those have a wider range in size than the middle layer. However, in case of the bottom layer the found polyester particle's major and minor dimensions are larger than the middle layer particles. So the evaluation of the particle size on its own is not enough to explain the plastic particles' retention mechanism.

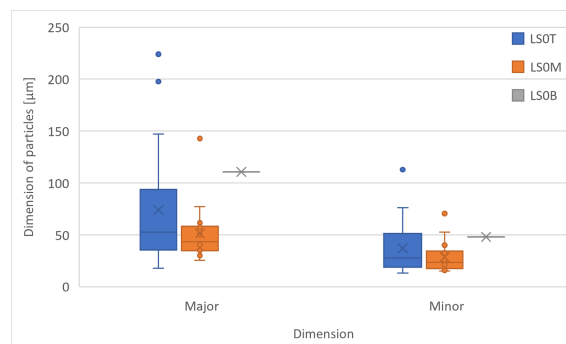
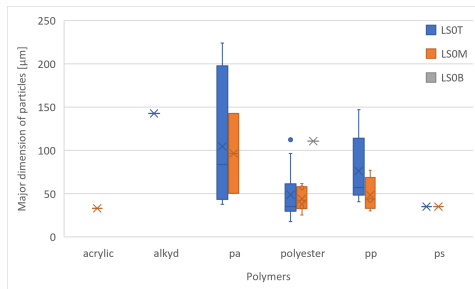


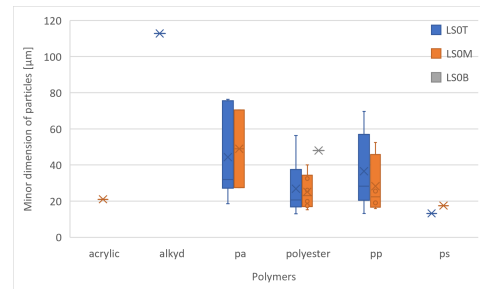
Figure 4.5: *Particle size distribution in the soil layers*

On Figure 4.6 the major and minor dimension of the particles can be seen by polymer type in order to evaluate the connection between the polymer size, type and position in the soil column.

Examining the particle size by polymer type, no further correlations can be seen per soil layer.



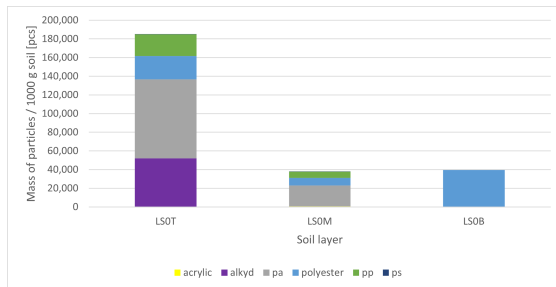
(a) The major dimension of the polymers in the soil layers by particle type



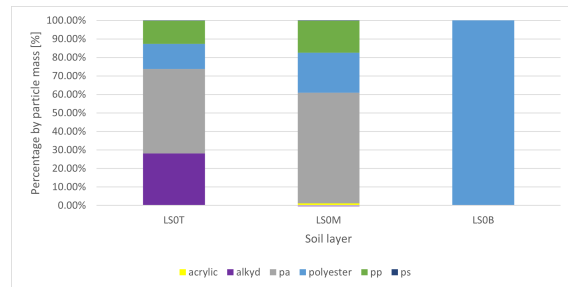
(b) The minor dimension of the polymers in the soil layers by particle type

Figure 4.6: Particle size distribution in the soil layers

Based on the measured major and minor dimension of particles, the volume of the different particle types was estimated. The volume values were used to calculate the mass of the different polymer types based on their respective density. On Figure 4.7a the particles mass dominance of the top layer can be seen. It means that the layer’s thickness is not the most important factor of the MP retention, because most of the particles are withheld in the top layer. On Figure 4.7b) the percentage of the mass of the polymers can be seen in the soil layers.



(a) The mass of the polymers in the soil layers



(b) The percentage of the mass of the polymers in the soil layers

Figure 4.7: Particle distribution in the soil layers based on the particle mass

4.3 Top soil samples abundance and polymer composition

To evaluate the retained plastic amount in the filter system’s top layer, the top soil samples were analysed. Figure 4.8 shows the average concentration and distribution of the polymers in the top soil samples. The dominance of the polypropylene is striking, the polyester, the polyamide and the polystyrene concentration is still visible but the rest is not noticeable.

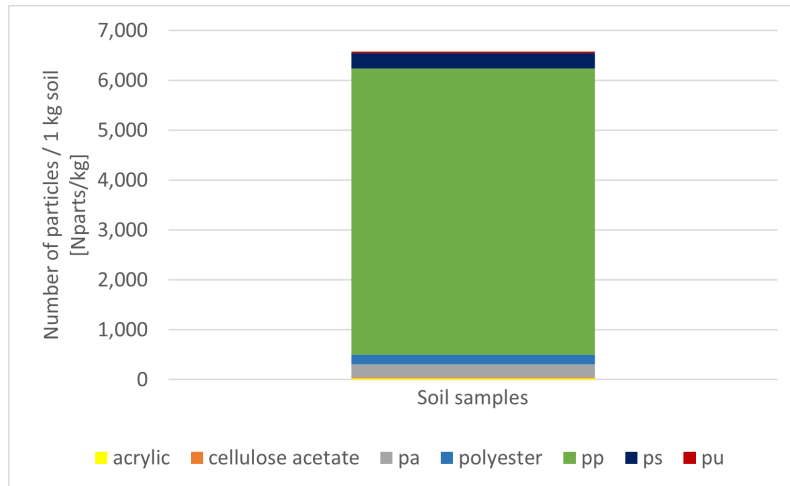
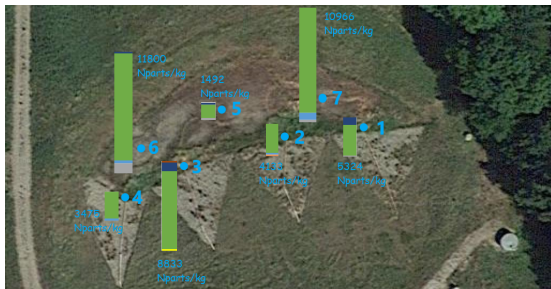


Figure 4.8: *The concentration of the MPs in the soil samples*

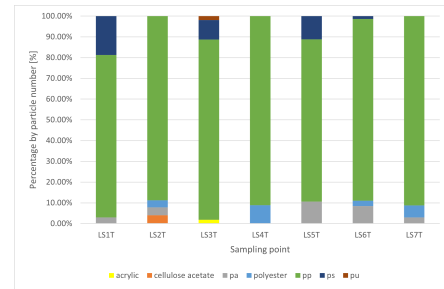
To see the results in more detail, Figure 4.9a shows the concentration (Npart/kg) of the particles per 1 kg top soil and Figure 4.9b shows the ratios of the polymer types by sampling point. Based on the large number of polyester ($\rho \sim 1.38 \text{ g} \cdot \text{cm}^{-3}$) on the filter installation, it can be assumed that there upward flow processes are present in the pre-basin, leading re-suspension of the settled high-density particles can thus be transferred to the soil filter. The differences in the particle concentration in the top soil layer can be traced back to the location of the discharge pipes and the sampling point distances form the outlet. The sample point location can be seen on Figure 3.2.

The largest concentration of particles (see Figure 4.9a) were found in case of sampling point no.6 and 7 (11,800 Npart/kg and 10,966 Npart/kg respectively), which are farther from the outlets. The high particle concentration may be due to the particles travelled in the water and were deposited further away from the pipe outlets. The exception was point no. 5 (1,492 Npart/kg) which is located farthest from the outlet points, between the points with the highest particle concentration. The concentration of the particles at the outlet points have similar values (no. 1: 5,324 Npart/kg, no. 2: 4,133 Npart/kg, no. 4: 3,475 Npart/kg) the exception is point no.3, where larger concentration of particles were found (8,833 Npart/kg). This may be because pipes close to the sampling points 1 and 2 are usually in use, so most of the particles travels with the water on the filter surface to the 3rd sampling point and are deposited there. In comparison with the results in Chapter 4.2, the concentration of the particles are higher in the top soil layer farther form the pipe outlet. This confirms the theory that the particles are transported by the surface water from the outlet point.

From polymer type point of view the dominance of the polypropylene particles is noticeable, this polymer type makes up 78.21- 91.19 % of the particles in the top soil samples. The most common particles next to the polypropylene are the polyamide particles with maximum 10.61 %, polyester with maximum 8.87 % and polystyrene with maximum 18.78 % ratio. Acrylic, cellulose acetate and polystyrene particles occur only once (see Figure 4.9). This result is differed from the soil layer evaluation (Chapter 4.2) where next to the polypropylene particles the polyester and polyamide particles appeared in large proportions. The difference can be traced back to the different sampling location and the distance from the pipe outlet.



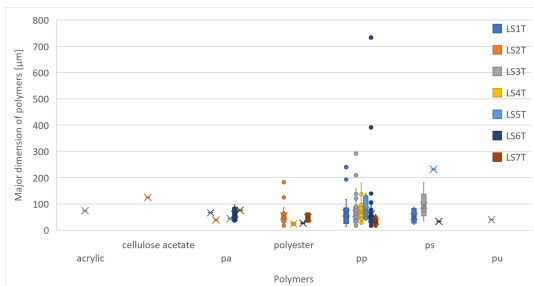
(a) The concentration (Npart/kg) of the polymers in the top soil samples



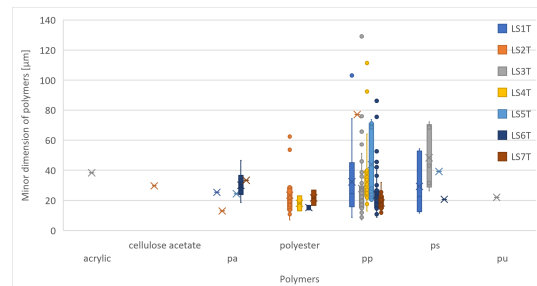
(b) The percentage of the polymers in the top soil samples

Figure 4.9: Particle distribution in the top soil samples based on the particle concentration (Npart/kg)

The particle retention depends on, not only the density but the dimension of the particles too. On Figure 4.10 can be seen the major and minor dimensions of the particles in the top layer. The samples were wet sieved with 500 μm sieves, but particles larger than 500 μm can also be noticed. However, the minor dimensions are smaller than 500 μm and in this way the particles could go through the sieve. The major and minor dimensions of particles in the top layer are similar that was found in Chapter 4.2 top soil layer. Significant differences were not found in the size of the different plastic types.



(a) The major dimension of the polymers in the top soil samples

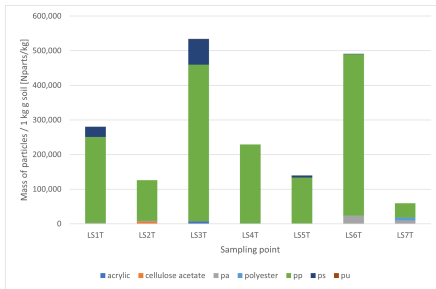


(b) The minor dimension of the polymers in the top soil samples

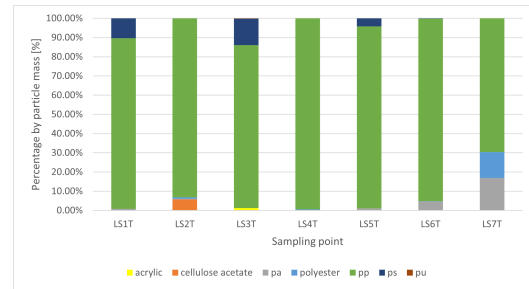
Figure 4.10: Particle size distribution in the top soil samples

As described in Chapter 4.2, the mass of the plastic contamination was calculated (see Figure 4.11). The largest mass of plastics was found in the sample from sampling point 3 and 6, which was expected based on the concentration of particles (see Figure 4.11a). However, in case of the sample from the sampling point 7, the concentration of the particles were large, while it has the smallest particle mass value. It means that the size of the particles were small which can be caused by the transportation related fragmentation or during the water transport, the larger particles were deposited earlier and only the smaller particles were travelled till the sampling point no. 7.

There is no relevant difference between the percentage distribution by concentration, mass and percentage mass of particles (see Figure 4.11b).



(a) The mass of the polymers in the top soil samples

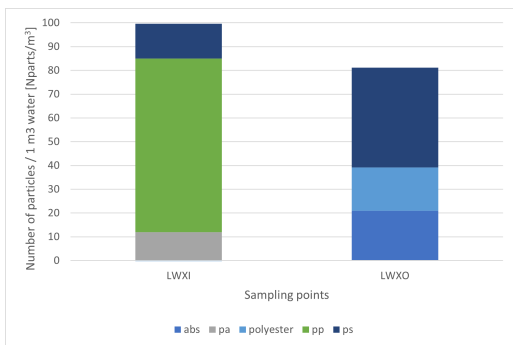


(b) The percentage of the mass of the polymers in the top soil samples

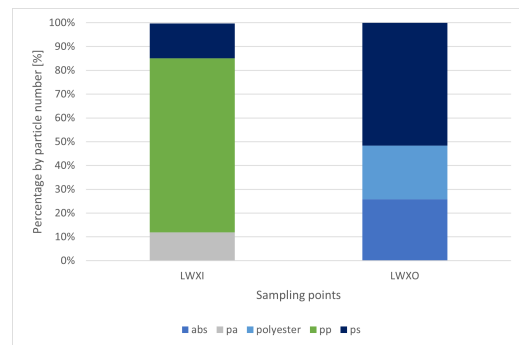
Figure 4.11: Particle distribution in the soil layers based on the particle mass

4.4 Comparison of water samples' results

As a result of the retained particles in the filter soil, the inlet and the outlet water samples were compared. In order to see the difference in the particle concentration differences, the sample results were converted to 1 m^3 of water and corrected with the blank results. The dataset of the particle distribution in the inlet and outlet samples can be seen on Figure 4.12.



(a) The concentration (Npart/ m^3) of the polymers in the water samples



(b) The percentage of the polymers in the water samples

Figure 4.12: Particle distribution in the water samples based on the particle concentration

In case of the inlet water, 3 polymer types were found: polyamide ($12\text{ Npart}/m^3$), polypropylene ($73\text{ Npart}/m^3$) and polystyrene ($15\text{ Npart}/m^3$). However, in the outlet water samples polyamide was not found, but abs was found ($21\text{ Npart}/m^3$) next to the polyester ($18\text{ Npart}/m^3$) and polystyrene ($42\text{ Npart}/m^3$) particles. Based on the Chapter 4.2 and Chapter 4.3, several types of polymers were retained by the filter soil system, such as acrylic, alkyd, cellulose acetate, polyamide, polyester, polypropylene and polyester. As a result of the filter soil system, the concentration of plastic particles was reduced and the polyamide content was filtered out. Plastic particles with a density higher than the water's density would normally have settled in the pre-basin, so they should only be present in small amounts on the filter soil. No regularity in the density of the filtered particles was observed.

Despite the large concentration of retained particles found in the soil samples, the particle concentration difference in the inlet and the outlet water shows low filtration efficiency. However, the high concentration of the particles in the outlet water might be due to the unusual, very sudden loading of the filter system with large amounts of water. So in normal conditions when the loading

is rain event related, more efficient retention can be expected. Furthermore, this large loading of the filters could have washed contamination from the filter out, contamination which might have been in place when the filters were constructed.

In order to find the reason of this retention, the sizes of the particles were compared (see Figure 4.13) from which it can be seen that the major and minor dimensions are slightly larger in the incoming water samples than in the outgoing water sample.

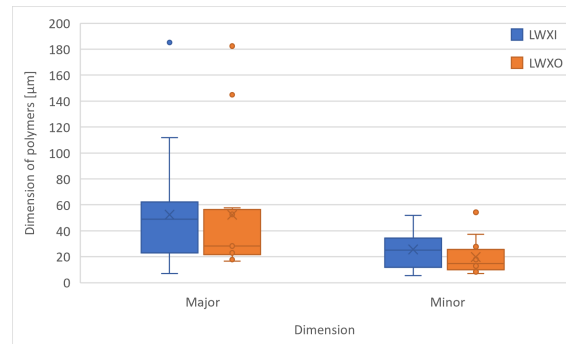
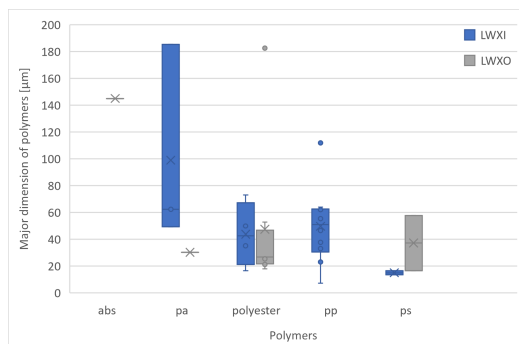
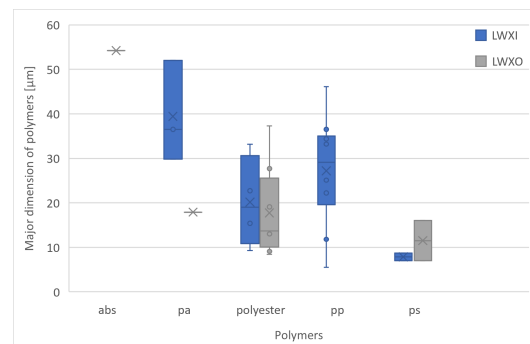


Figure 4.13: *The major and minor dimension of the polymers in the water samples*

The particle size was evaluated as a function of polymer type, but no regularity was observed, but the major and minor dimension of the different particle types are in similar size range (see Figure 4.14).



(a) The major dimension of the polymers in the water samples

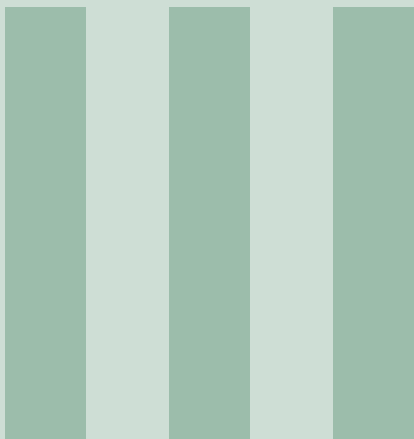


(b) The minor dimension of the polymers in the water samples

Figure 4.14: *Major and minor dimensions of the particles in the water samples*

4.5 Follow-up experiment

Since the properties of the road wear car tire particles were taken into account during the density separation process, these particles can be detected by the gas chromatography method.



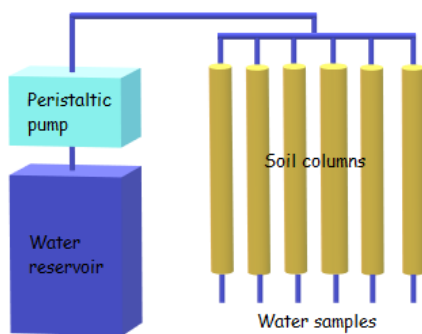
Filter soil experiment

5	Experimental method	35
5.1	Experimental setup	
5.2	Column preparation	
5.3	The experiment	
6	Materials and methods	37
6.1	Materials	
6.2	Sample processing	
6.3	Identification and quantification	
7	Results and discussion	43
7.1	Polymer distribution by column	
7.2	Polymer distribution by polymer type	
7.3	Polymer distribution by size	
7.4	Follow-up experiment	

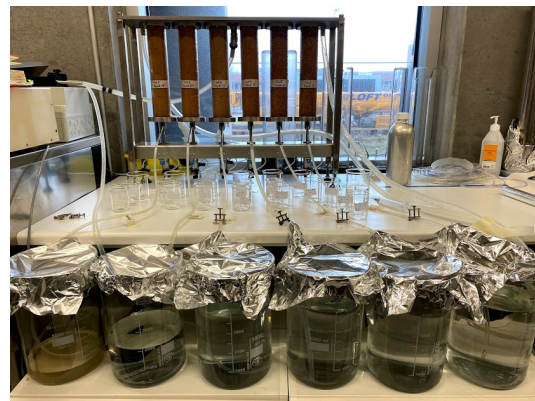
5. Experimental method

5.1 Experimental setup

The columns were installed to a custom-made stand where the 5 μm filtered water was pumped from a metal water reservoir through a peristaltic pump (see Figure 5.1). The water flowing through the sand column was collected in 2 litres beakers and then, filtered on a 10 μm mesh.



(a) Experimental setup sketch



(b) The column experimental setup

Figure 5.1: Major and minor dimensions of the particles in the water samples

5.2 Column preparation

In order to have plastic free soil, the sand was muffled. The determination of the soil volume (588.75 cm^3) was performed with the measurement of the experimental column inner diameter (5cm) and length (30cm). To determine the exact amount of required soil quantity, the dry bulk density (ρ_b) was defined as 1.5 g DM/cm^3 soil and the gravimetric soil-water content of the room temperature soil was determined with a Mettler Toledo Moisture Analyzer HE73.

The experimental columns were filled up in four parts (see Figure 5.2). Thereafter, a bottom part with 300 μm filter was placed at the bottom of the column to prevent the soil getting loose. After that, the first part of the soil (quarter of the total mass) was measured out with a scale and then a funnel was used to put the soil into the column. The next step was to compress the soil to achieve the 7.5 cm height marking line.

The soil surface was prepared prior to measuring the next sample, the smooth surface was disturbed for better connection of the layers. The

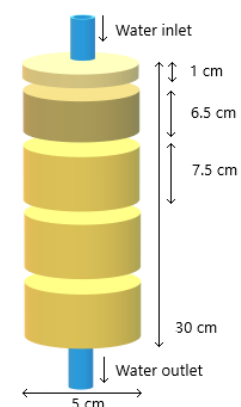


Figure 5.2: Sketch of the columns

next step was to weigh the second part of the soil (quarter of the total mass), fill it into the column and hammer it to achieve the column's 15 cm mark with the soil surface. This measuring and hammering process was performed with the third quarter of soil, and this way filled up the column until the 22.5 cm line. The last quarter was divided into two parts, the column was filled up to reach the 29 cm mark and the last 1 cm was left empty.

The prepared columns were inserted into the experimental setup and the drain hole was closed. In order for the particles to be properly placed in the sand column, a 1 cm deep hole was dug in the centre of the sand column. After that, the counted particles were poured and flushed into the hole. The hole and the last 1 cm of the column was filled with clean muffled soil.

5.3 The experiment

During the experiment, the amount of water flowing through the columns was calculated based on the Danish climate standard precipitation. The climate standard was defined as 791.9 mm based on the collected precipitation data from 1981 to 2010 [DMI, 2021]. The climate standard was multiplied with the reduction factor to calculate the amount of runoff. The reduction factor represent that the small rains do not run off, which causes $\sim 35\%$ loss of the annual rain.

$$791.9 \text{ mm/year} \cdot 0.65 = 514 \text{ mm/year} = 0.514 \text{ m/year}$$

The filter system was designed with 200 m² filter surface per reduced hectare of catchment area (10000 m²). Based on the calculated ratio (10000 m² / 200 m² = 50), it means that each year 1 m² filter soil receives water from 50 m² of catchment area [Vollertsen et al., 2018a]. With this ratio the volume of water flowing through the 1 square meter soil filter in one year was calculated.

$$50 \text{ m}^2 \cdot 0.514 \text{ m} = 25.7 \text{ m}^3$$

Based on the dimensions of the used experimental columns (5 cm diameter) the surface area was calculated: 0.00196 m². To represent one year precipitation through the experimental column, 50 litres of filtered water was used.

$$0.00196 \text{ m}^2 \cdot 25.7 \text{ m} = 0.05 \text{ m}^3$$

The setup was loaded at the same time and passed through the 50 liters. The duration of the experiment was depended on the flow rate, which depends on the properties of the soil. Column 4 was the fastest with about 4 hours, Column 3, 5 and 6 between 6-8 hours, Column 2 around 17 hours and Column 1 was the slowest with an experimental period of about 53 hours.

The effluent was collected in a 2 liters beaker dedicated to the column and then filtered through a dedicated filtration unit and 10 μm mesh filter. At the end of the experiment, the dedicated beaker was rinsed and the water used for rinsing was also filtered with the column dedicated filter.

6. Materials and methods

6.1 Materials

6.1.1 Filter soil mixtures

The soil texture determines how porous the soil system and therefore how fast water flows through it and what size of particles can pass through depending on the pore size. This property is depending on the fractions of coarse and fine sand, alongside clay, silt and organic matter. While the sand fraction, which makes up the largest portion of the composite it is the finer particles provide direct retention and cleaning properties to the soil and determine the hydraulic conductivity and therefore infiltration capacity [Loll & Moldrup, 2002].

To evaluate the retention ability of microplastic particles, the soil types shown in Table 6.1 were examined. Sand types were selected based on the particle size and the particle size range. As the number of columns increases, the increase in the smallest and largest particle size can be seen. The upper limit of the particle size was set to 2 mm because those are removed during sample processing.

Table 6.1: *Experimental column setup*

	Sand %	Type	Size
Column1	100	Stoberisand_18	0.09-0.25 mm
Column2	100	Stoberisand_29	0.18-0.50 mm
Column3	100	Stoberisand_40	0.25-0.71 mm
Column4	100	Filtersand_0	0.40-0.80 mm
Column5	100	Filtersand_2	0.71-1.29 mm
Column6	100	Filtersand_3	0.90-1.6 mm

The ranges of the grain sizes are known, but sieving was performed to determine the particle size distribution of the different type of sands (see Figure 6.1). In addition, the sieving analysis allows to construct columns with precise contents of coarse sand, fine sand and clay in order to isolate and evaluate the potential influence of each on the hydraulic properties and particle retention of the resulting column.

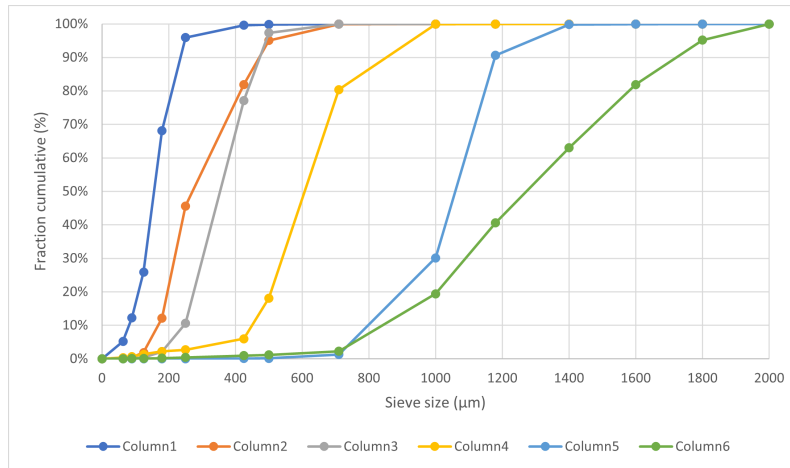


Figure 6.1: The grain size distribution curves of the sands

Based on the soil particle size, the pore size can be calculated, where the quarter of the particle size is equal to the pore size [Loll & Moldrup, 2002]. However, in case of different particle sizes, it should be taken into consideration that even smaller particles can be in the pores, thus reducing the pore size. This process can increase the particle retention capability of the soils with various grain sizes. On Table 6.2 the ratio of the different grain sections can be seen. It is noticeable that the Column 5 and 6's grain size distribution are uniform and the most varied particle sizes are shown at the first column.

Table 6.2: Soil fractions - description of the columns can be seen in table 6.1. CS = Coarse Sand (%), FS = Fine Sand (%), Bottom frac = Bottom fraction of sieving tower (%)

	Column1	Column2	Column3	Column4	Column5	Column6
CS frac	0.32	0.88	0.98	0.98	1.00	1.00
FS frac	0.63	0.12	0.02	0.02	0.00	0.00
Bottom frac	0.05	0.00	0.00	0.00	0.00	0.00

6.1.2 Plastic particle types and quantities

In order to examine the particle density effect on retention, particles of different densities were selected. PS with density 1.05 g/cm^3 was chosen to represent the plastic particles with the density around the water density. Of the higher density materials, PA (1.31 g/cm^3) and PVC (1.38 g/cm^3) were selected. The difference in density between PA and PS is minimal, but their shape is different, so the effect of shape on retention can be examined with it. PS particles have a regular spherical shape, while PA particles have an irregular shape. The particles sizes are between $40\text{-}80 \text{ }\mu\text{m}$ which is suitable for further tests with an FTIR machine.

In order to add a known number of particles to the columns, the different type of particles were counted with FlowCam 8000 Series Dynamic Imaging Particle Analyzer (Fluid Imaging Technologies, INC).

The FlowCam is an imaging flow cytometer which combines the technologies of the flow cytometer and an imaging microscope. As a result, it can count, capture and save digital images of the particles in a fluid stream [FIT, 2017].

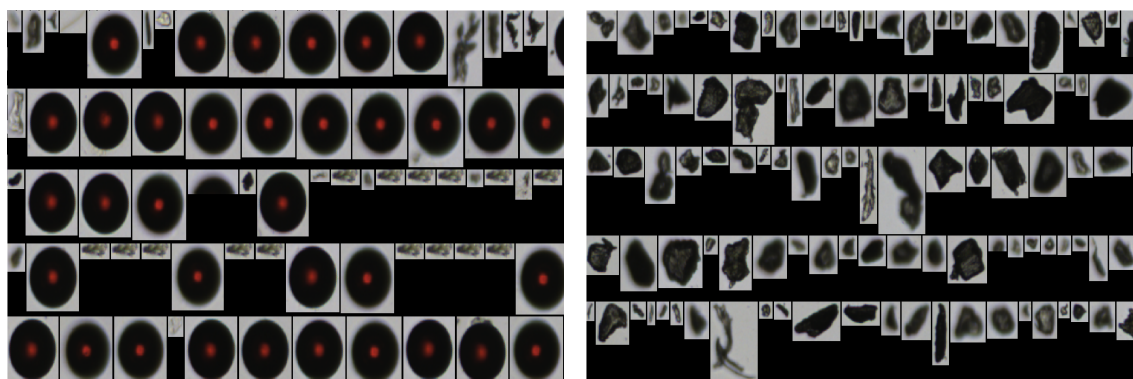
The Objective lenses and the Flow Cells were used according to the particle sizes. The magnification of the objective is inversely proportional to the diameter of the flow cell as well as the diameter of

the largest particle being examined [FIT, 2017]. In case of the PVC particles, Objective 10X was used with FV100 Flow Cell, which cause difficulties during the counting and imaging process and the Flow cell was clogged several times. Due to the clogging issues, the 4X lens and FV100 Flow Cell were used for the PS and PA particles. The flow rate and the number of images were set to reach the highest efficiency with FlowCam VisualSpreadsheet software (see the setup and settings on Table 6.3).

Table 6.3: *The setup and the settings of the FlowCam*

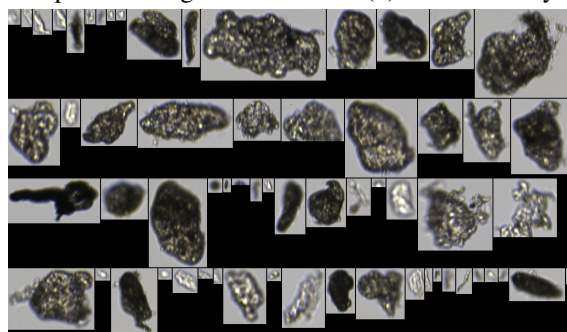
	Objective	Flow Cell	Flow rate [ml/min]	No. of image [frames/sec]	Efficiency [%]
PS	4X	FV300	1.00	9	72.4
PVC	10X	FV100	0.66	98	72.4
PA	4X	FV300	1.00	9	72.4

After the setup, the focus and the cleaning of the Flow Cell was performed. A blank sample was taken prior to sample handling to ensure that cross-contamination was avoided. As a result of the particle counting can be seen on Figure 6.2 where the differences of the particle shapes by polymer type can be seen. The presence of contaminants is most striking among PS particles, as PS particles has circular shape. The images captured by the machine were then sorted automatically and manually to remove any contaminants.



(a) Unsorted Polystyrene particle images

(b) Unsorted Polyamide particle images



(c) Unsorted Polyvinyl-chloride particle images

Figure 6.2: *FlowCam images*

In addition to the counted particle amount, an efficiency value is required to determine the amount of microplastic in the material. The efficiency depends on the flow cell, the objective, the flow rate and the captured number of images. The efficiency is calculated automatically by the VisualSpreadsheet software based on the non-visualised portion of the field. [Poulton & Martin, 2010].

$$\text{Amount of microplastic} = \text{Counted particles} \cdot \text{Efficiency} \quad (6.1)$$

Aliquots thus prepared containing a known amount of particles were distributed as evenly as possible in the soil columns so that the different particle numbers and the total number of particles within each column did not differ significantly (see Table 6.4)

Table 6.4: The number of different particles per coulumn

	Column1	Column2	Column3	Column4	Column5	Column6
PVC [pcs]	268	334	452	402	383	204
PS [pcs]	325	195	188	278	254	202
PA [pcs]	347	215	211	184	203	133

6.2 Sample processing

The collected water flowed through the columns were filtered with 10 μm mesh sized metal filter. The soil in the column was divided into 3 equal parts (see Figure 6.3).



Figure 6.3: Divide the amount of soil in the column into three parts

Thus, a total of 6 water samples and 18 soil samples were generated from the 6 experimental columns. Appendix A shows the source and the ID of the sample where the same identification number system was followed as in Chapter 3.1.2.

The general overview of the soil sample preparation can be seen on Figure 6.4, the process steps are described in Chapter 3.2.1.

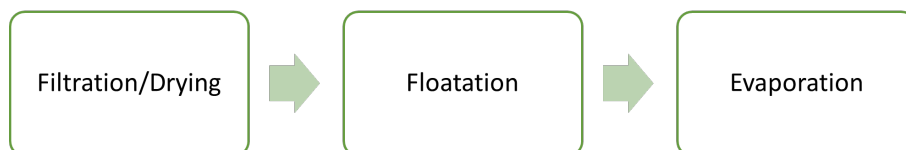


Figure 6.4: The column experimental setup

As the plastic particles properties are known, in order to be on the safe side from density point of view, in case of the flotation step, the samples were processed with an SPT solution of $1,7 \text{ g} \cdot \text{cm}^{-3}$ density. After evaporation, the vial was filled with 2 ml HPLC grade 50% EtOH in order to have a more concentrated sample for deposition.

6.3 Identification and quantification

The samples were analysed in the same way, the same method and machine was used as described in Chapter 3.3.1. During the analysis, specific reference spectra was used where only the polymers used in the preparation of the columns were included.

7. Results and discussion

7.1 Polymer distribution by column

For proper evaluation, the data should be examined in their entirety without any breakdown. It can be seen from Figure 7.1 that most of the particles remain in the upper soil layer for columns 1 (GS: Grain Size: 0.09-0.25 mm) and 5 (GS: 0.71-1.29 mm). However, the most important aspect is to avoid the introduction of plastic particles into the water, which was only the case with Column 5 (GS: 0.71-1.29 mm). Based on this, the column with the most effective plastic retention is Column 5 (GS: 0.71-1.29 mm). The columns' soil composition can be seen on Figure 6.1 and Table 6.1 and the grain size ranges can be seen right after the column ID number in parentheses.

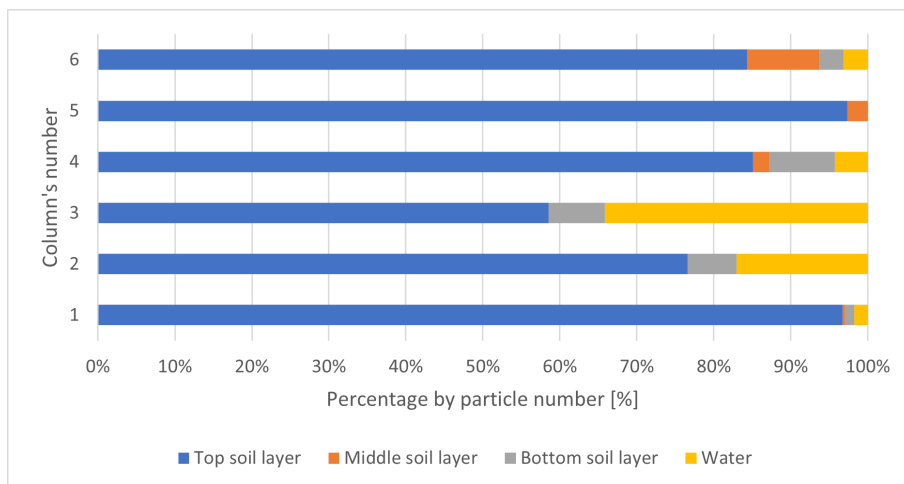


Figure 7.1: Total polymer distribution in the soil and water samples per column

7.2 Polymer distribution by polymer type

For a more detailed evaluation, to see the different polymer types distribution in the soil layers and the water samples, the percentage by particle number was visualised.

Figure 7.2 shows the polystyrene distribution in the soil and water samples. In case of Column 2 (GS: 0.18-0.50 mm), no polystyrene particles were present in the samples. This was probably due to the fact that the samples were examined once, there was no possibility of re-examination. For the other columns, the highest proportion of polystyrene particles was found in the upper soil layer. Only Column 4 (GS: 0.40-0.80 mm) had polystyrene particles in the water sample (18 %), and Column 1 (GS: 0.09-0.25 mm) had lower polystyrene particles in the bottom soil sample (3 %) and the water sample (4 %). Based on the analysis of polystyrene particles with a density close to water, no clear difference in retention can be established between the columns, except for the slightly weaker performance of columns 1 (GS: 0.09-0.25 mm) and 4 (GS: 0.40-0.80 mm).

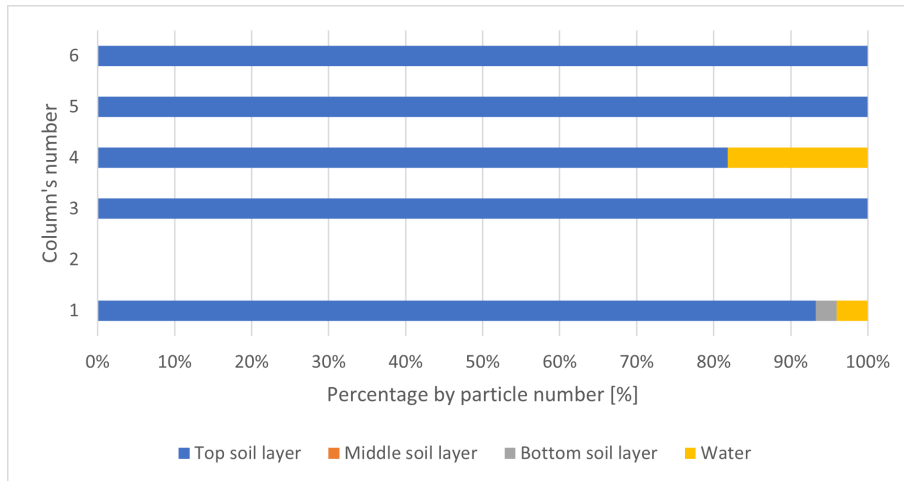


Figure 7.2: *Polystyrene distribution in the soil and water samples per column*

On Figure 7.3 the polyamide particles distribution can be seen in the experimental columns. It is clear that most of the particles are retained in the top soil layer, similar to that observed with retention of polystyrene particles. However, differences can be observed between the columns. The polyamide particles were retained in the highest proportions in Column 5 (GS: 0.71-1.29 mm) (97 %) and Column 1 (GS: 0.09-0.25 mm) (98 %). The lowest proportion of retention in the top layer was found in Column 3 (GS: 0.25-0.71 mm) with 45 %. In the case of columns 4 (GS: 0.40-0.80 mm) (3 %), 5 (GS: 0.71-1.29 mm) (3 %) and 6 (GS: 0.90-1.6 mm) (12 %), a small proportion of particles also appeared in the middle soil layer. The middle layers in the other columns did not contain polyamide. The polyamide presence in the bottom layer is minimal, no more than 10 %. The polyamide content of the water samples differs depending on the particle retention capacity of the columns. The column with the best particle retention based on the evaluation of polyamide particles was column number 5 (GS: 0.71-1.29 mm), as there were no polyamide particles in either the lower soil layer or the water sample. However, columns 1 (GS: 0.09-0.25 mm), 4 (GS: 0.40-0.80 mm), and 6 (GS: 0.90-1.6 mm) were also effective in retaining particles, with only minimal amounts of polyamide being found in the bottom layer and the water sample.

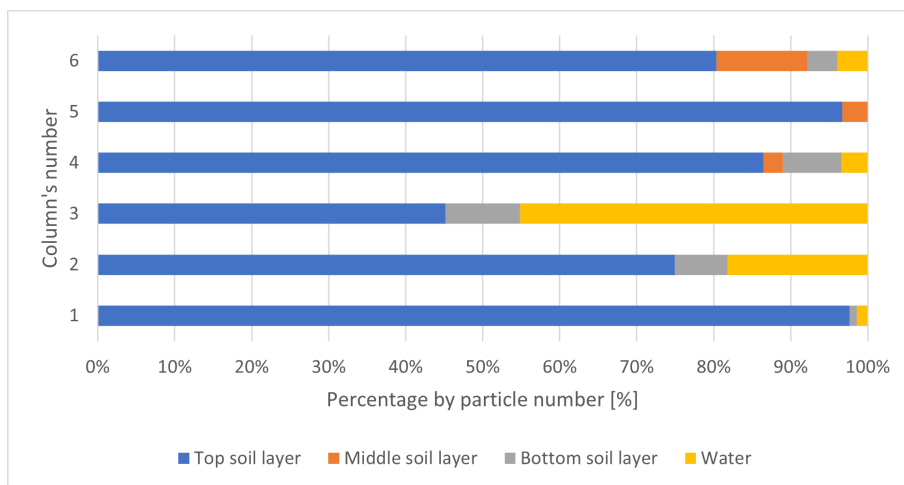


Figure 7.3: *Polyamide distribution in the soil and water samples per column*

In case of the PVC particles distribution (see Figure 7.4) similar retention is observed as for polystyrene. Exception for columns 1 (0.09-0.25 mm) and 4 (0.40-0.80 mm), only particles in the upper soil layer were found. In case of Column 1 (0.09-0.25 mm), there was a PVC particle in the middle soil layer (2 %), and in the case of column 4 (0.40-0.80 mm), there was a PVC particle in the bottom soil layer (25 %). PVC did not appear in the water sample for any of the columns.

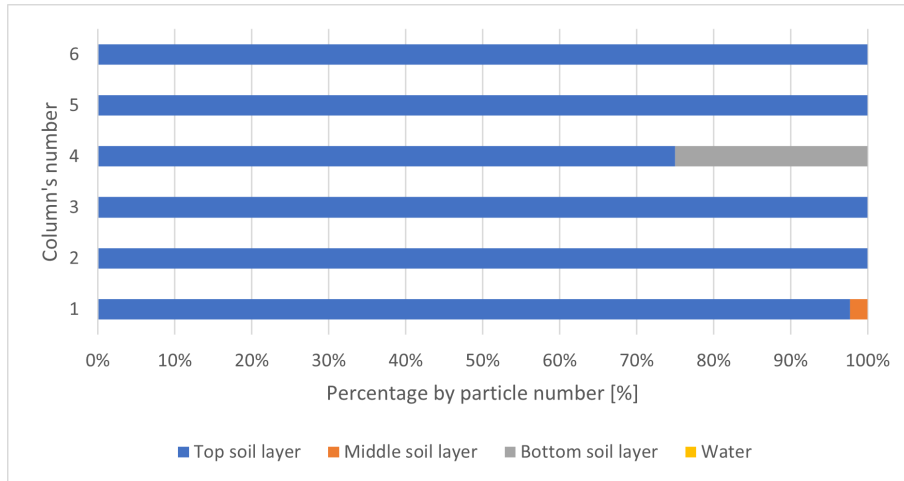


Figure 7.4: Polyvinyl-chloride distribution in the soil and water samples per column

7.3 Polymer distribution by size

The plastic particle size distribution in the soil layers were examined in order to see the particle transport in the soil as a function of particle size. As shown in Figure 7.5, no significant difference in the size of the plastic particles in the different layers was observed.

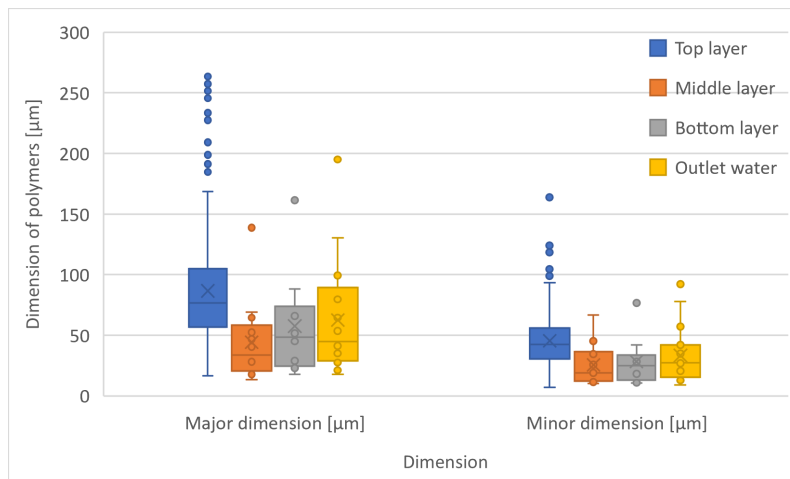
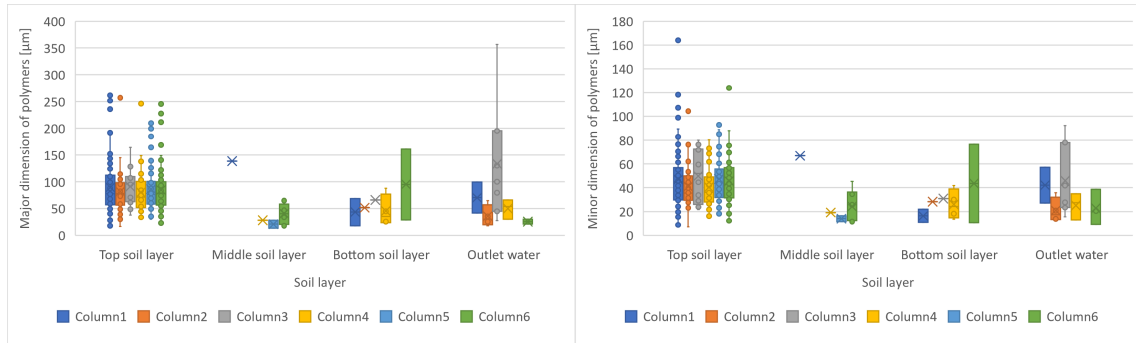


Figure 7.5: Major and minor dimensions of the particles in the soil layers

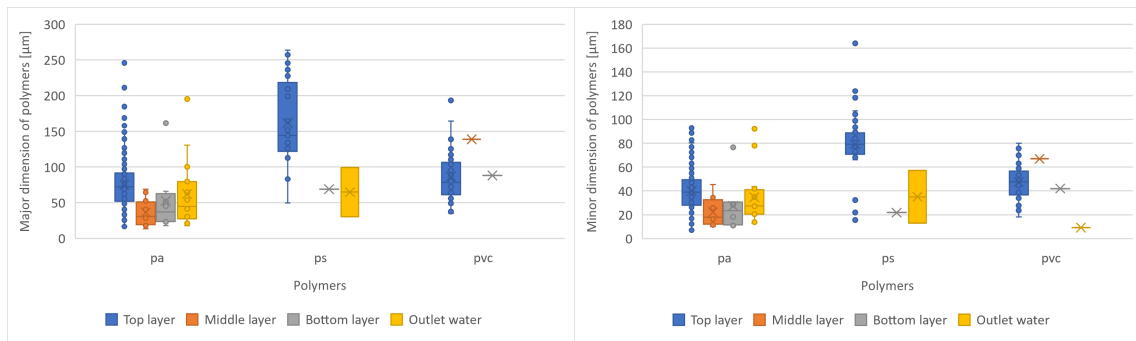
In order to get a more detailed picture of the particles retained in the different soil layers and to find a correlation between the particle permeability of the column and the particle size of the soil, smaller and larger dimensions of the retained particles were also plotted for each column (see Figure 7.6). The results do not show a clear relationship between soil particle size and retained plastic particles.



(a) The major dimension of the polymers in the soil layers (b) The minor dimension of the polymers in the soil layers

Figure 7.6: Major and minor dimensions of the particles in the soil layers

In order to investigate whether there is a difference between plastic particles of different sizes and different properties, the particle size distribution was also plotted by material type. Based on Figure 7.7, it can be seen that large differences and patterns are not visible.



(a) The major dimension of the polymers in the soil layers (b) The minor dimension of the polymers in the soil layers

Figure 7.7: Major and minor dimensions of the particles in the samples by particle type

7.4 Follow-up experiment

For a more accurate result, more depositions and scans should be done and the experiment with sand columns should be repeated.

As a continuation of the experiment, an additional 6 columns were prepared in which 5 % peat was added to the same soils, thus examining the effect of the addition of organic matter on retention, as organic matter generates aggregates, so microplastic retention is expected to be more effective. The preparation of the added particles and the flow of 50 litres of water through the soil mixture was performed with the same way as described in Chapter 6, followed by the complete sample preparation process described in Section 3.2.1.

However, problems arose during the second density separation, which could not be solved by several troubleshooting procedures. The material to be separated floated together with the plastic particles, the amount of sample did not decrease with further hydrogen peroxide treatment, nor did it sink to the bottom of the separation funnel with a slight decrease in the density of the SPT solution. Replacing the SPT solution with a $1.7 \text{ g} \cdot \text{cm}^{-3}$ ZnCl solution finally solved the problem, the organic matter residues sank to the bottom of the separation funnel, making the clear sample available. However, no further sample preparation steps were made due to time limitations. As a result, sample preparation was not completed, so results from the resulted 24 soil samples and 6 water samples are not displayed.

IM Conclusion & Reflection

8	Conclusion	51
8.1	Filter installation	
8.2	Filter soil experiment	
9	Bibliography	55
A	Experimental sample IDs	59

8. Conclusion

8.1 Filter installation

Soil samples and water samples were taken to evaluate the retention of microplastic particles in the filter installation in Låsby. At one sampling point, the filter soil was sampled to its full depth, where 3 different layers were distinguished, thus, the vertical particle distribution was examined. The samples were purified with multi-step sample preparation before FPA-FTIR-imaging spectroscopy analysis. As a result of the sample analysis, it can be concluded that the amount of microplastic decreases with increasing depth. Figure 8.1 (Figure 4.4) shows that the sample from the topsoil contains the highest concentration of MP, while in the bottom layer sample the lowest concentration was found. This means that the MPs does not travel to the deeper soil layers in the soil and peat mixture. Even though the results are blank corrected, the source of the polymer content in the bottom layer can still be contributed the external contamination.

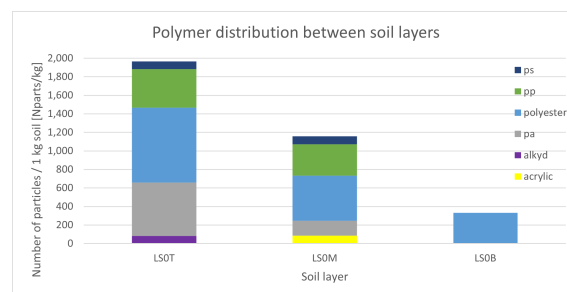


Figure 8.1: *The concentration of the polymers in the soil layers*

The polymer distribution was also examined in terms of polymer type and particle size. Based on the evaluation, the size of the particles has no effect on its location in the soil layer.

At another 7 points, the upper soil layer was sampled, so we got a overview of the horizontal distribution of the particles. Based on the evaluation in Figure 8.2a (Figure 4.8) and the Figure 8.2b (Figure 4.12a), the soil-filter basin retains microplastic pollution from the incoming wet basin pre-treated road water. However, the difference between the inlet and outlet water shows only 17 % removal rate. The water samples were examined to find patterns in retention, but no regularity in the density and size of the filtered particles was observed.

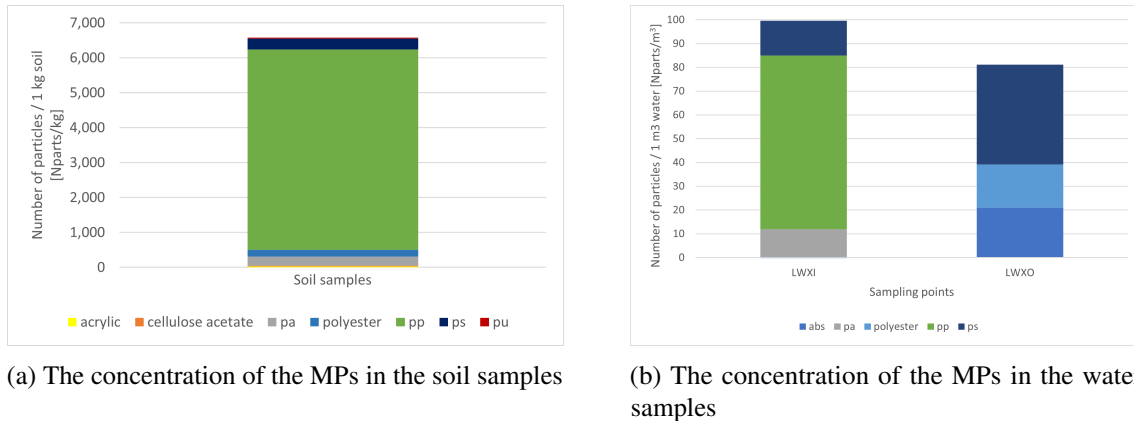


Figure 8.2: Particle distribution in the soil layers based on the particle mass

Despite the small percentage of removal, a large amount of microplastic accumulation was found in the soil samples (see Figure 4.8). This means that the soil filter effectively restrains the spread of microplastics. Seven different polymers were found in the soil samples, where polypropylene was present the largest proportion.

The number of the particles in the top soil layer samples were evaluated in function of the location of the sampling point. It was found that the particles are transported by water from the pipe outlet, so the water dynamics defines the proportion of retained particles per sampling point. Furthermore, it was found that the amount of polypropylene was dominant at each sampling point.

Examination of the blank samples shows that contamination must be prevented as much as possible during sampling and sample processing in order to ensure that the samples, and in particular the results of pure samples such as water samples, can be used. In case of the soil sample the contamination rate is only 0.5 % but in case of the most sensitive water samples, the ratios are 34 % (inlet water) and 41 % (outlet water).

8.2 Filter soil experiment

Counted plastic particles were used to investigate the retention capability of soils with different grain sizes. To acquire the grain size distribution curve of the different soils, the soils were sieved. In order to add a known amount of plastic particles to the experimental columns, the particles were counted with FlowCam. The chosen particles for spiking were PA, PVC and PS in order to use plastics of different shapes and densities in the size range $\sim 40\text{-}80\ \mu\text{m}$. During the experiment, to represent one year precipitation, 50 litres of filtered water was used. After the experiment, the samples were prepared and examined with FTIR machine. The results were evaluated a library of infrared spectra, which was created by analysis of reference materials.

Based on the experimental results, differences can be seen in the retention capacity of different sands. Figure 8.3 (Figure 7.1) shows the distribution of the plastic particles in the soil layers and in the water samples. Based on this, Column 3 (0.25-0.71) is the least efficient and Column 5 (0.71-1.29) is the most efficient in retaining plastic particles.

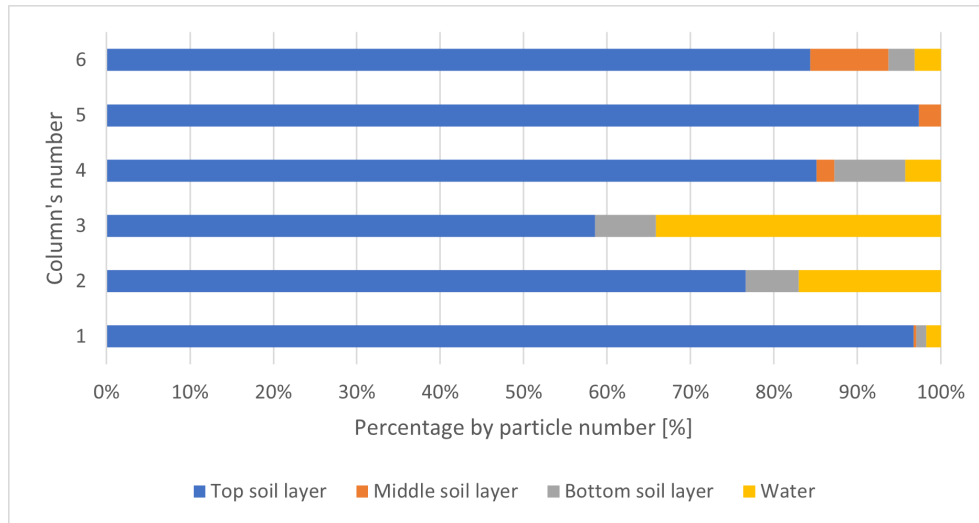


Figure 8.3: Total polymer distribution in the soil and water samples per column

The retention capability was evaluated based on polymer type, size and shape. It was found that the least efficiently retained particle type was polyamide (1.31 g/cm^3) and the retention of polystyrene (1.05 g/cm^3) and polyvinyl-chloride (1.38 g/cm^3) was similarly effective.

In addition, the minimal thickness of soil layer can be determined. In case of the most efficient soil column (no. 5) there no particles were observed in the bottom layer, so the smallest filter soil thickness in order to retain the microplastic particles should be at least 20 cm.

9. Bibliography

- ACD-GRI, 2019.** ACD-GRI. *Environmental and Health Risks of Microplastic Pollution*. European Commission, Directorate-General for Research and Innovation, Unit RTD.DDG1.02 - Scientific Advice Mechanism, B-1049 Brussels, 2019. ISBN ISBN 978-92-76-02425-5. doi: doi:10.2777/65378. Scientific Opinion 6/2019.
- Avio et al., 2017.** Carlo Giacomo Avio, Stefania Gorbi & Francesco Regoli. *Plastics and microplastics in the oceans: From emerging pollutants to emerged threat*. Marine Environmental Research, pages 2–11, 2017. doi: <https://doi.org/10.1016/j.marenvres.2016.05.012>. <https://www.sciencedirect.com/science/article/pii/S0141113616300733>.
- DMI, 2021.** DMI. *Klimanormaler for Danmark*, 2021. <https://www.dmi.dk/vejarkiv/normaler-danmark/>.
- Fang & Qu, 2018.** Xu Fang & Yinbo Qu. *Microbial Production and Application*. Springer, Singapore, 152 Beach Road, 21-01/04 Gateway East, Singapore 189721, Singapore, 2018. ISBN 978-981-13-0749-2 and 978-981-13-4491-6. doi: <https://doi-org.zorac.aub.aau.dk/10.1007/978-981-13-0749-2>.
- FIT, 2017.** FIT. *FlowCam® 8000 Series Dynamic Imaging Particle Analyzer User Guide*, 2017. Fluid Imaging Technologies.
- Horton et al., 2017.** Alice A. Horton, Alexander Walton, David J. Spurgeon, Elma Lahive & Claus Svendsen. *Microplastics in freshwater and terrestrial environments: Evaluating the current understanding to identify the knowledge gaps and future research priorities*. Science of The Total Environment, 586, 127–141, 2017. ISSN ISSN 0048-9697. doi: <https://doi.org/10.1016/j.scitotenv.2017.01.190>. <https://www.sciencedirect.com/science/article/abs/pii/S0048969717302073>.
- Klöckner et al., 2019.** Philipp Klöckner, Thorsten Reemtsma, Paul Eisentraut, Ulrike Braun, Aki Sebastian Ruhl & Stephan Wagner. *Tire and road wear particles in road environment – Quantification and assessment of particle dynamics by Zn determination after density separation*. Chemosphere, 222, 714–721, 2019. doi: <https://doi.org/10.1016/j.chemosphere.2019.01.176>. <http://www.sciencedirect.com/science/article/pii/S004565351930195X>.
- Kurien et al., 2019.** Kurien, Biji T. & R. Hal. *Scofiel*. Springer Science+Business Media, 233 Spring Street, New York, NY 10013, U.S.A., 2019. ISBN 978-1-4939-8792-4. doi: <https://doi.org/10.1007/978-1-4939-8793-1>. URL https://doi.org/10.1007/3-540-27382-4_1.
- Liu et al., 2019.** Fan Liu, Kristina Borg Olesen, Amelia Reimer Borregaard & Jes Vollertsen. *Microplastics in urban and highway stormwater retention ponds*. Science of The Total Environment, 671, 992–1000, 2019. ISSN 0048-9697. doi: <https://doi.org/10.1016/j.scitotenv.2019.03.416>. <https://www.sciencedirect.com/science/article/pii/S0048969719314226>.

- Loll & Moldrup, 2002.** Per Loll & Per Moldrup. *Soil Characterization and Polluted Soil Assessment*. 2002.
- Löder et al., 2017.** Martin G. J. Löder, Hannes K. Imhof, Maike Ladehoff, Lena A. Löschel, Claudia Lorenz, Svenja Mintenig, Sarah Piehl, Sebastian Primpke, Isabella Schrank, Christian Laforsch & Gunnar Gerdts. *Enzymatic Purification of Microplastics in Environmental Samples*. *Environmental Science Technology*, 51, 14283–14292, 2017. doi: 10.1021/acs.est.7b03055. <https://pubs-acsc-org.zorac.aub.aau.dk/doi/abs/10.1021/acs.est.7b03055>.
- Munsterman & Kerstholt, 1996.** Dirk Munsterman & Susan Kerstholt. *Sodium polytungstate, a new non-toxic alternative to bromoform in heavy liquid separation*. *Review of Palaeobotany and Palynology*, 91, 417–422, 1996. doi: [https://doi.org/10.1016/0034-6667\(95\)00093-3](https://doi.org/10.1016/0034-6667(95)00093-3).
- Poulton & Martin, 2010.** Nicole J. Poulton & Jennifer L. Martin. *Imaging flow cytometry for quantitative phytoplankton analysis - FlowCAM*. United Nations Educational, Scientific and Cultural Organization, 7, Place de Fontenoy, 75352, Paris 07 SP, 2010. Intergovernmental Oceanographic Commission of UNESCO.
- Primpke et al., 2020.** Sebastian Primpke, Richard K. Cross, Svenja M. Mintenig, Marta Simon, Alvise Vianello, Gunnar Gerdts & Jes Vollertsen. *Toward the Systematic Identification of Microplastics in the Environment: Evaluation of a New Independent Software Tool (siMPle) for Spectroscopic Analysis*. *SAGE journals*, 74, 2020. doi: <https://doi.org/10.1177/0003702820917760>.
- Rasmussen et al., 2021.** Lasse Abraham Rasmussen, Lucian Iordachescu, Susanne Tumlin & Jes Vollertsen. *A Complete Mass Balance for Plastics in a Wastewater Treatment Plant Macroplastics Contributes more than Microplastic*. *Water Research*, 2021. ISSN 0043-1354. doi: <https://doi.org/10.1016/j.watres.2021.117307>.
- Redondo-Hasselerharm et al., 2020.** P. E. Redondo-Hasselerharm, G. Gort2, E. T. H. M. Peeters & A. A. Koelmans. *Nano- and microplastics affect the composition of freshwater benthic communities in the long term*. *Science Advances*, 2020. <http://advances.sciencemag.org/>.
- Rist et al., 2020.** Sinja Rist, Alvise Vianello, Mie Hylstoft Sichelau Winding, Torkel Gissel Nielsen, Rodrigo Almeda and Rocío Rodríguez Torres & Jes Vollertsen. *Quantification of plankton-sized microplastics in a productive coastal Arctic marine ecosystem*. *Environmental Pollution*, 266, 2020. ISSN 0269-7491. doi: <https://doi.org/10.1016/j.envpol.2020.115248>. <https://www.sciencedirect.com/science/article/pii/S0269749120338902>.
- Tagg et al., 2017.** A. S. Tagg, J. P. Harrison, Y. Ju-Nam, a M. Sapp, C. J. Sinclair E. L. Bradley & J. J. Ojeda. *Fenton's reagent for the rapid and efficient isolation of microplastics from wastewater*. *Chem. Commun.*, 53, 372–375, 2017. doi: 10.1039/c6cc08798a. <https://doi-org.zorac.aub.aau.dk/10.1039/C6CC08798A>.
- Tiseo, 2021.** Ian Tiseo. *Global plastic production 1950-2019*, 2021. <https://www.statista.com/statistics/282732/global-production-of-plastics-since-1950/>.
- Vollertsen et al., 2018a.** Jes Vollertsen, Niels Krogh Kristensen & Nikki van Alst. *Driftserfaringer med filteranlæg til efterpolering af vejevand*. TRAFIK VEJE, 2018.
- Vollertsen et al., 2018b.** Jes Vollertsen, Niels Krogh Kristensen & Nikki van Alst. *Etablering af filteranlæg til efterpolering af vejevand*. TRAFIK VEJE, 2018.

-
- Wagner et al., 2014.** Martin Wagner, Christian Scherer, Diana Alvarez-Muñoz, Xavier Bourrain Nicole Brennholt, Sebastian Buchinger, Elke Fries, Cécile Grosbois, Jörg Klasmeier, Teresa Marti, Sara Rodriguez-Mozaz, Ralph Urbatzka, A Dick Vethaak, Margrethe Winther-Nielsen & Georg Reifferscheid. *Microplastics in freshwater ecosystems: what we know and what we need to know*. Environmental Sciences Europ, 2014. doi: 10.1186/s12302-014-0012-7. <https://doi.org/10.1186/s12302-014-0012-7>.
- Xiao et al., 2016.** Juan Xiao, Chuan Wang, Shushen Lyu, Hong Liu, Chengchun Jiang & Yangming Lei. *Enhancement of Fenton degradation by catechol in a wide initial pH range*. Separation and Purification Technology, 169, 202–209, 2016. ISSN 1383-5866. doi: <https://doi.org/10.1016/j.seppur.2016.04.031>. <http://www.sciencedirect.com/science/article/pii/S1383586616302131>.
- Zazo et al., 2011.** Juan A. Zazo, Gema Pliego, Sonia Blasco, Jose A. Casas & Juan J. Rodriguez. *Intensification of the Fenton Process by Increasing the Temperature*. Industrial engineering chemistry research, 50, 866–870, 2011. doi: <https://doi-org.zorac.aub.aau.dk/10.1021/ie101963k>. <https://doi-org.zorac.aub.aau.dk/10.1021/ie101963k>.

A. Experimental sample IDs

Table A.1: *The experimental samples' ID according to the sample location, sample type, sampling point and sample source.*

Sample ID	Location	Type	Sampling point	Source
ES1T	Experiment	Soil	Column 1	Top layer: 0-10 cm
ES1M	Experiment	Soil	Column 1	Middle layer: 10-20 cm
ES1B	Experiment	Soil	Column 1	Bottom layer: 20-30 cm
EW1	Experiment	Water	Column 1	50 litres
ES2T	Experiment	Soil	Column 2	Top layer: 0-10 cm
ES2M	Experiment	Soil	Column 2	Middle layer: 10-20 cm
ES2B	Experiment	Soil	Column 2	Bottom layer: 20-30 cm
EW2	Experiment	Water	Column 2	50 litres
ES3T	Experiment	Soil	Column 3	Top layer: 0-10 cm
ES3M	Experiment	Soil	Column 3	Middle layer: 10-20 cm
ES3B	Experiment	Soil	Column 3	Bottom layer: 20-30 cm
EW3	Experiment	Water	Column 3	50 litres
ES4T	Experiment	Soil	Column 4	Top layer: 0-10 cm
ES4M	Experiment	Soil	Column 4	Middle layer: 10-20 cm
ES4B	Experiment	Soil	Column 4	Bottom layer: 20-30 cm
EW4	Experiment	Water	Column 4	50 litres
ES5T	Experiment	Soil	Column 5	Top layer: 0-10 cm
ES5M	Experiment	Soil	Column 5	Middle layer: 10-20 cm
ES5B	Experiment	Soil	Column 5	Bottom layer: 20-30 cm
EW5	Experiment	Water	Column 5	50 litres
ES6T	Experiment	Soil	Column 6	Top layer: 0-10 cm
ES6M	Experiment	Soil	Column 6	Middle layer: 10-20 cm
ES6B	Experiment	Soil	Column 6	Bottom layer: 20-30 cm
EW6	Experiment	Water	Column 6	50 litres